International Journal of Geosciences, 2015, 6, 1285-1316
Published Online December 2015 in SciRes. http://www.scirp.org/journal/ijg
http://dx.doi.org/10.4236/ijg.2015.612103

Present Velocity Field in the Italian Region by GPS Data: Geodynamic/Tectonic Implications

Enzo Mantovani[1], Marcello Viti[1], Nicola Cenni[2], Daniele Babbucci[1], Caterina Tamburelli[1]

[1]Dipartimento di Scienze Fisiche, della Terra e dell'Ambiente, Università degli Studi di Siena, Siena, Italy
[2]Dipartimento di Fisica ed Astronomia, Università degli Studi di Bologna, Bologna, Italy
Email: marcello.viti@unisi.it

Received 18 November 2015; accepted 26 December 2015; published 29 December 2015

Abstract

The analysis of geodetic observations carried out by 478 continuous GPS stations in the Italian region since 2001 has allowed a fairly good definition of the ongoing horizontal velocity field with respect to Eurasia. It is argued that such evidence can provide important insights into the geodynamic context in the central Mediterranean area. Numerous velocity vectors in the Apulia zone coherently indicate that the southern Adriatic domain is moving roughly NE ward. Since no significant decoupling zone between this domain and Nubia has so far been recognized, one could expect that the kinematics of these two plates is compatible. However, this condition is not fulfilled if the Nubia-Eurasia relative motion is taken from the global kinematic models, either deduced by long-term evidence [1] or short-term geodetic data [2] [3]. This problem is considerably reduced if the alternative Nubia-Eurasia rotation pole suggested by [4] is taken into account. This choice is also suggested by other major long-term evidence in the Mediterranean region. The numerous geodetic vectors available in two Adriatic sectors, the Apulia zone and the Venetian plain, would imply an Adria-Eurasia rotation pole incompatible with all Nubia-Eurasia Eulerian poles so far proposed. Since a significant relative motion between these plates is not compatible with the absence of a tectonic decoupling zone, we suppose that the short-term kinematics of Adria might be influenced by a transient non-rigid behaviour of that plate. This hypothesis is compatible with the expected effects (post seismic relaxation) of the major decoupling earthquakes that have occurred along Periadriatic zones in the past tens of years. The compatibility of the GPS kinematic pattern in the Apennine belt, Calabria Arc and Sicily with the implications of the geodynamic/tectonic interpretations so far proposed for the central Mediterranean area is then discussed.

Keywords

Geodesy, Geodynamics, Italy, Central Mediterranean

How to cite this paper: Mantovani, E., Viti, M., Cenni, N., Babbucci, D. and Tamburelli, C. (2015) Present Velocity Field in the Italian Region by GPS Data: Geodynamic/Tectonic Implications. *International Journal of Geosciences*, **6**, 1285-1316. http://dx.doi.org/10.4236/ijg.2015.612103

1. Introduction

It is widely recognized that the evolution of the Mediterranean area has been considerably influenced by the convergence between Africa and Eurasia. However, the fact that major extensional processes, such as the formation of relatively large back-arcbasins, have developed in the Mediterranean region during its Neogene evolution has led some authors to suppose that the convergence of the surrounding plates is not the unique driving mechanism. In particular, it has been suggested that the gravitational sinking of subducted lithosphere (slab roll-back) has considerably contributed to the above processes [5]-[7]. This last hypothesis has been confuted by some authors [8]-[14], who suggest that the Neogene deformation pattern in that area can plausibly and coherently be explained as an effect of the motion of Nubia (sensu [1]) and the Anatolian-Aegean-Balkan system with respect to Eurasia.

The spreading of opinions about the geodynamic setting in the Mediterranean region is significantly influenced by the fact that the relative motion between Nubia and Eurasia is not uniquely recognized yet. Uncertainty mainly concerns the trend of such plate convergence and the configuration and kinematics of the Adriatic plate. Global kinematic models based on the analysis of long-term evidence (late Pliocene-Quaternary North Atlantic mid-oceanic ridge spreading rates and transform fault azimuths, [1] [15] [16]) suggest that at Mediterranean latitudes Nubia moves roughly NW to NNW ward with respect to Eurasia. Global models inferred from short-term space geodesy data [2] [3] provide a Nubia-Eurasia relative motion with direction more oriented towards the west [17].

However, as argued by [4], the above convergence trend can hardly be reconciled with several major features of the Quaternary deformation pattern in the whole Mediterranean region, which rather suggests a NNE ward orientation of such plate convergence.

To explain why the Nubia-Eurasia pole provided by global kinematic models may be not reliable, [4] point out that the plate configuration adopted by such analyses is oversimplified, since it involves a two plates model (Nubia and Eurasia), notwithstanding that the distribution of seismic and tectonic features in the interposed regions suggests the presence of two independent microplates (Morocco and Iberia). This possibility is particularly interesting since the NNE ward trend of the Nubia-Eurasia relative motion suggested by Mediterranean constraints can be also reconciled, within errors, with the North Atlantic kinematic constraints, if the proposed four plates configuration (**Figure 1**) is taken into account [4].

In this work, we point out some aspects of the space geodetic (GPS) velocity field in the Italian area that can provide significant constraints on the Nubia-Eurasia relative motion, and the kinematics of other important structures in the central Mediterranean area, such as the Adriatic plate (Adria), the Apennine belt and the Calabrian and Hyblean wedges.

2. GPS Network and Data Processing

The space geodetic (GPS) observations obtained from 478 continuous stations operating in the Italian area and surroundings over the period January 1, 2001 April 30, 2015 have been considered in order to estimate the present horizontal kinematic field.

The phase and pseudo-code data for each station have been analyzed by the GAMIT software version 10.5 [18] adopting a distributed procedure [19], as described by [20] [21]. The whole network has been divided into 43 clusters, following a simple geographic criterion, while maintaining the shortest baseline as possible. Loose constraints (100 m) have been assigned to the daily position coordinates of each station belonging to all clusters. The International GPS service for Geodynamics (IGS) precise orbital solutions from Scripps Orbit and Permanent Array Center have been included in the processing with tight constraints, such as the Earth Orientation Parameter. The daily loosely constrained solutions have been combined into a unique solution by the GLOBK software [22], and aligned into the ITRF2008 reference frame [3] by a weighted six parameters transformation (three translations and three rotations), using the ITRF2008 coordinates and velocities of the 13 high-quality common IGS stations shown in the inset of **Figure 2**.

Then, the time series have been analyzed to estimate the north, east and vertical components of the geographical position of each site, following the procedure described by [20] [21]. Only the sites with a minimum length of 2.5 years have been included in the processing in order to avoid biases generated by unreliable estimated seasonal signals [23] and/or by rate uncertainties, due to short time series [24]. As argued in several papers [24]-[28], the noise in time series can be described as a power law process.

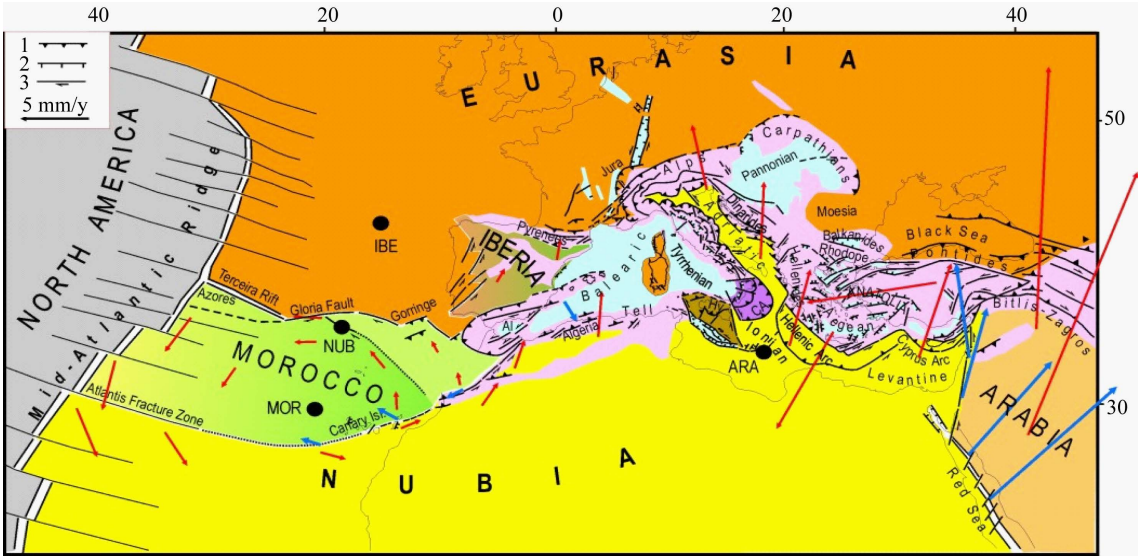

Figure 1. Plate configuration and long-term (Quaternary) kinematic pattern in the Mediterranean region provided by [4]. Black dots identify the location of the proposed Euler poles of the Arabia (ARA), Iberia (IBE), Morocco (MOR) and Nubia (NUB) plates with respect to Eurasia. Red arrows indicate the motions of the above plates with respect to Eurasia predicted by the respective Euler poles and the motion of the Anatolian-Aegean system. Blue arrows along plate borders show the relative motion of the Morocco and Arabia plates with respect to Nubia. CA = Calabrian wedge (violet), Hy = Hyblean wedge (brown). The velocity field shown in the Anatolian-Aegean system is compatible with geological evidence (see [8]-[10] [14]). See [4] for details about the configuration and kinematics proposed for the easternmost part of the Morocco plate (light green). Main orogenic belts are pink. 1, 2, 3: Compressional, extensional and transcurrent features.

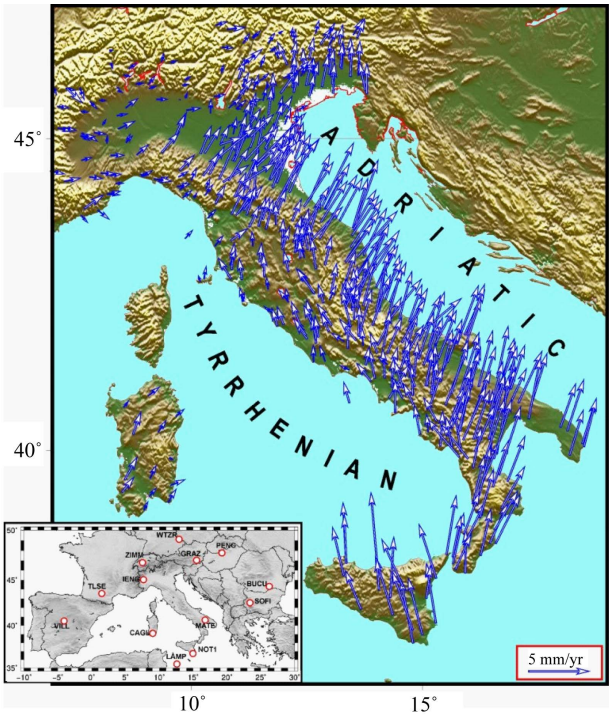

Figure 2. Horizontal velocities (blue vectors) of the GPS sites with respect to a fixed Eurasian frame (Euler pole at 54.23˚N, 98.83˚W, ω = 0.257˚/Myr [3]). The inset shows the location of the 13 IGS stations that have been used to align the daily solutions of the network to the ITRF 2008 references frame [3].

Different methods have been developed to characterize noise in GPS time series and its impact on velocity uncertainties [26] [27] [29] [30]. We have used the reformulated computation method of the Maximum Likelihood Estimation introduced by [30] in order to estimate the characteristics of the noise and the realist uncertainties associated with velocity values. The resulting ITRF2008 horizontal velocity vectors with respect to the adopted Eurasian frame [3] are reported in the **Appendix** and mapped in **Figure 2**.

3. Possible Tectonic Implications of the Geodetic Velocity Field

3.1. Southern Adria Kinematics and Nubia-Eurasia Relative Motion

The velocity field shown in **Figure 2** clearly indicates that the Apulia zone (Southeastern Italy), certainly belonging to the southern Adriatic domain [31] [32], is moving roughly NE ward, with a rate of about 4 - 5 mm/year. This evidence is fairly robust since it is coherently indicated by more than 20 velocity vectors and is consistent with the indications provided by the analysis of earthquake focal mechanisms in Periadriatic zones [33]-[35]. If Nubia were moving roughly NNW to NW ward, as predicted by global kinematic models, it would be necessary to identify an active decoupling zone between Nubia and Adria.

Attempts at identifying such decoupling have been made by several authors [33] [35]-[44]. However, the considerable spreading of the solutions so far proposed (**Figure 3**), concerning location, trend and tectonic nature of the presumed decoupling zones, clearly underlines the ambiguity of the available evidence, as pointed out by

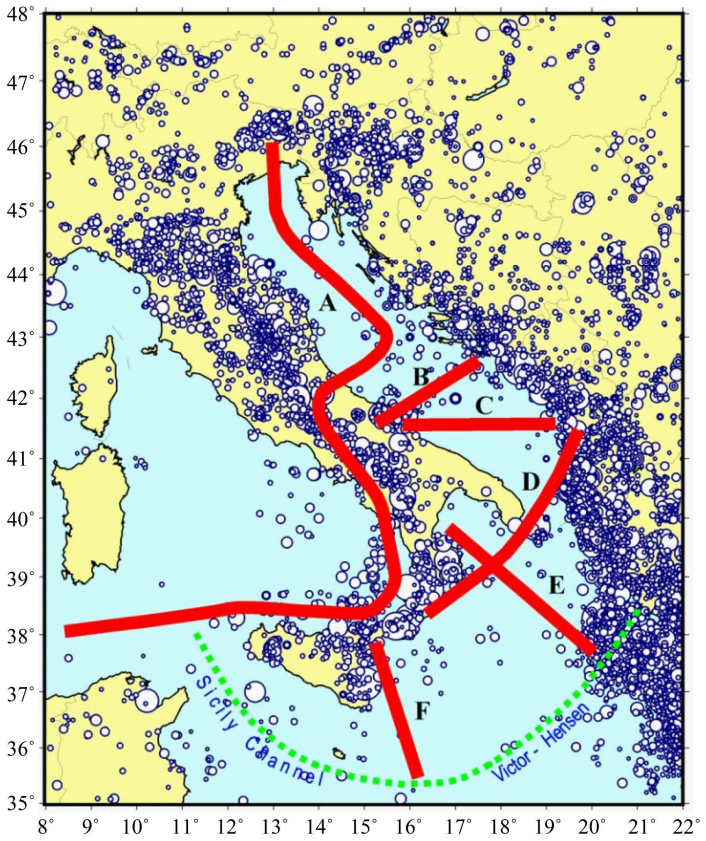

Figure 3. Distribution of major seismicity (M ≥ 5.0) in the Adriatic domain and surroundings from 1600 [48] [49] and configuration of the decoupling zones between the Adria and Nubia domains proposed by a) [40]; b) [35] [36] [44]; c) [37] [38]; d) [33]; e) [41] [43]; f) [39]. The dotted green line indicates the fault systems (Sicily Channel and Victor Hensen) that, following [10], have decoupled the Adriatic-Ionian plate from Nubia since the Late Miocene (with a considerable slowdown of the relative motion since the middle Pleistocene).

some authors [17] [45] [46]. The most significant evidence about the lack of a clearly recognizable decoupling zone between Nubia and Adria is given by the low level of seismicity in the presumed decoupling zones (**Figure 3**) and by the fact that none of them correspond to a major active fault system cutting through the Adria domain [46] [47].

The major difficulty pointed out above cannot simply be ignored. Since the kinematics of southern Adria seems to be well defined, one should carefully check the reliability of the Nubia-Eurasia relative motion provided by global kinematic models [1]-[3]. As argued earlier, a detailed discussion about this problem is given by [4] [14], who have proposed an alternative hypothesis about the Nubia-Eurasia convergence (**Figure 1**). This solution should seriously be taken into account since does not involves any major difficulty. First of all, the proposed Nubia-Eurasia relative motion is compatible with southern Adria's geodetic field, and thus does not require the frustrating search of an unlikely decoupling zone. Furthermore, such kinematic model can be reconciled with major Mediterranean and North Atlantic kinematic constraints, as described by [4].

The above kinematic solution has been criticized by [2], who do not recognize the Iberia and Morocco independent microplates hypothesized by [4]. As concerns Iberia, [2] postulate that no significant relative motion between that domain and Eurasia is taking place at the Pyrenean collision zone, in particular the 1.5 mm/y convergence rate implied by the [4] model. However, it is difficult to believe that such small relative motion can be ruled out for a boundary zone where significant seismic activity takes place (**Figure 4**), and several compressional and traspressional active faults have been identified (e.g., [50] [51]). For instance, [50] estimate that in the western Pyrenees the roughly E-W Lourdes thrust alone may accommodate up to 0.25 mm/yr of N-S convergence. So, it can hardly be excluded that seismic and/or aseismic fault slip at the whole Pyrenean tectonic boundary may accommodate the above mentioned convergence rate.

[2] also suggest that seismotectonic activity in western Iberia could not account for the Iberia-Eurasia relative motion predicted by [4]. However, recent works [52] confirm that such zone is dissected by a number of active NNE-striking faults, whose slip rates could reach 0.8 mm/yr, which roughly matches the amplitude of the Iberia-Eurasia relative motion predicted by [4]. In our opinion, the fact that both the boundary zones between the presumed Iberia plate and Eurasia are affected by significant seismicity (**Figure 4**) cannot easily be reconciled with a null relative motion between such plates. Another problem raised by [2] is the fact that some predictions of the [4] model are not compatible with the geodetic velocities of 3 geodetic sites in Iberia (Ebro, Madrid, Ybes, **Figure 4**). In this case as well, the difference between observed and predicted velocities is of the order of 1 mm/y, that may be compatible with the possible uncertainty of GPS data.

[2] also recall that magnetic lineations in the North Atlantic have been interpreted as an evidence that Iberia has moved as part of Eurasia in the last 10 My [53]. However, one must be aware that spreading rates at the North Atlantic ridges are mainly influenced by the motion component of Atlantic domains perpendicular to

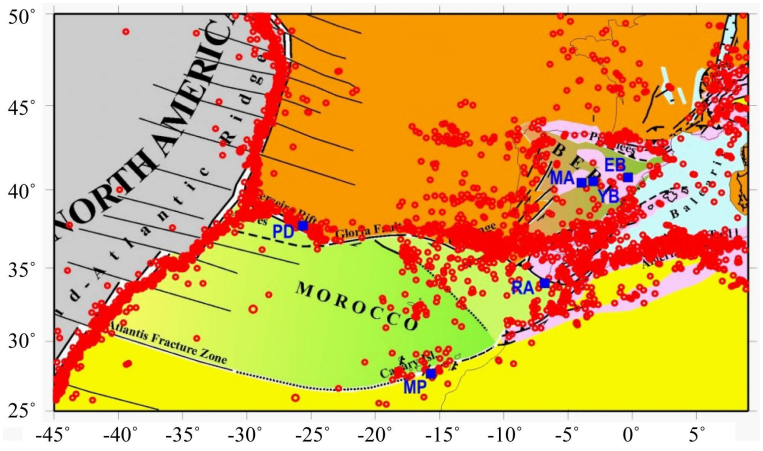

Figure 4. Seismicity distribution in the Western Mediterranean and central Atlantic region (M ≥ 4.0, 1970-2015) from the database of the Incorporated Researcher Institutions for Seismology (IRIS), available at http://ds.iris.edu/ds/nodes/dmc/data//.EB, MA, YB, MP, PD, RA indicate the location of the Ebro, Madrid, Ybes, Mas Palomas, Ponta Delgada and Rabat GPS stations.

ridges (mainly oriented E-W), and that consequently the presumed roughly N-S relative motion (1.5 mm/y) between Eurasia and Iberia can hardly produce significant effects on spreading rates at those ridges.

Moreover, [13] suggest that the actual Iberia microplate considerably differs from the previous Atlantic-Iberia plate. Indeed, since the late Miocene the Iberia microplate decoupled from the oceanic sector located between the Mid Atlantic Ridge and the Portugal fault system, which became part of Eurasia [13].

As concerns the Morocco microplate, [2] point out a discrepancy between the predictions of the Morocco-Nubia pole provided by [4] and the geodetic velocities at Mas Palomas (**Figure 4**). However, it must be considered that such site lies along an active tectonic boundary zone (as recognized by [2] and that consequently the real meaning of such observation cannot easily be recognized. [2] also suggest discrepancies between the predictions of the [4] Morocco-Eurasia pole and the geodetic velocities in the Ponta Delgada and Rabat sites (lying inside the presumed Morocco microplate). However, the entities of such discrepancies are compatible with the possible uncertainty of geodetic data.

[2] also remark that the strike-slip motion provided by [4] at the Atlantis-Canary Islands fracture zone (taken as the southern boundary of the presumed Morocco microplate) is not compatible with the lack of seismicity. However, it must be considered that the section of that fracture going through the Canary Islands has been affected by considerable tectonic, seismic and volcanic activity [54]. It is worth noting that [55] adopted the plate configuration suggested by [4], involving an independent Morocco microplate bounded by the Atlantis-Canary Islands fracture zone, to explain the magmatic processes that developed in the Canary Islands. As concerns the sector of that fracture zone lying west of the Canary Islands, one should consider that reliable information about seismic activity may only be available for the last tens of years. Anyway, it is worth noting that most of the current volcanic activity of the Canary Islands, often associated with earthquake swarms [56], occurs near the El Hierro island, which is the youngest volcanic complex of the archipelago, located at the eastern edge of the fracture zone envisaged by [4].

[57] point out that the results of statistical tests involving three GPS sites located in the Canary Islands (LPAL, GMAS and MAS1) confute the necessity of the independent Morocco microplate proposed by [4]. However, the same authors admit that the stations located in Morocco (RABT, IFRN and TETN) show residual velocities (with respect to the Nubia-Eurasia motion) exceeding 1 mm/y, suggesting that Morocco may not be rigidly coupled with Nubia.

To tentatively explain the difference between the Nubia-Eurasia kinematic models derived by geodetic data and geological evidence, [2] argue that the kinematics of the plate involved is changed in the short-term. However, this hypothesis may weaken the objections of such authors about the discrepancies they claim between the predictions of the [4] long-term kinematic model and some geodetic velocities.

As last, one could recall that the plate configuration of the first long term global kinematic model (NUVEL-1 [15]) is significantly different from the last one (MORVEL [2]), which involves a number of new microplates. In particular, recent works ([2] [57]) suggest that the Somalia and Lwandle microplates are probably independent from the former Africa plate, whereas the eastern boundary of the original Eurasian plate could be a complex mosaic formed by the Amur, Okhotsk, Yangtze and Sundaland microplates, along with other minor blocks. Such fragmentation of lithospheric domains, once believed to be very large coherent plates, may encourage the scientific community to make a more accurate check of the plate configuration proposed by [4].

3.2. Adria Plate?

The GPS velocity field shown in **Figure 2** provides information about the present kinematics of two zones certainly belonging to the Adria continental domain (**Figure 5**). One is Apulia, as discussed in the previous point, and the other is the Venetian plain, *i.e*. the Adria foreland area which underthrusts the eastern Southern Alps [32]. This evidence is very significant since it is coherently indicated by a relatively high number (more than 20 in both zones) of subparallel velocity vectors.

If Adria were assumed to behave as a rigid independent plate, the two geodetic constraints mentioned above would imply an Adria-Eurasia rotation pole roughly located in the Western Alps. This result, compatible with the ones previously obtained by the analysis of earthquake slip vectors in Periadriatic zones [33] [35] [36], would mean that Adria does not move in close connection with Nubia, whatever Nubia-Eurasia pole is considered among the ones so far proposed. However, such conclusion can hardly be reconciled with the lack of a clear active decoupling zone between Adria and Nubia. Thus, we rather suppose that the short-term evidence (either

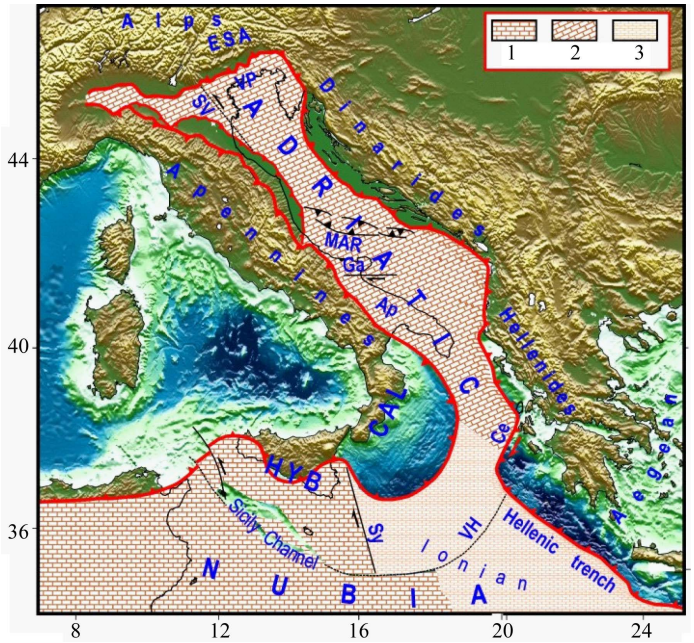

Figure 5. Sketch of major structural domains in the Central Mediterranean area. 1-2) African and Adriatic continental domains, 3) Oceanic Ionian domain, Other symbols as in **Figure 1**. A description of the previous tectonic phases that have led to the present configuration of the Adriatic plate and surrounding belts is given in **Figure 5** and the related comments in the text. AP = Apulia, CAL = Calabrian wedge, Ce = Cefalonia fault system, ESA = Eastern Southern Alps, Ga = Gargano, HYB = Hyblean wedge, MAR = Mid Adriatic ridge, SV = Schio-Vicenza fault system, Sy = Siracusa fault system, VH = Victor Hensen fault system, VP = Venetian Plain.

geodetic data or/and earthquake slip vectors) refers to a transient non-rigid behaviour of the Adria domain. This effect may be due to the peculiar distribution of seismic decouplings that have occurred in the Periadriatic boundary zones during the last tens of years. For investigating this problem we have taken into account the evidence and arguments presented by [49] [58] [59], which suggest that major seismicity in the Periadriatic zones tends to undergo a progressive northward migration through the eastern (Dinarides) and western (Apennine) boundary zones, up to reach the northern front of the Adria plate (Eastern Southern Alps).

The analysis of the post 1400 seismic histories of the Periadriatic zones has allowed the above authors to recognize a number of migrating seismic sequences, each lasting about 200 years [49] [58]. The last presumably complete sequence has probably developed until about 1920-1930. In the successive sequence (still ongoing, **Figure 6**), major Periadriatic earthquakes have mainly occurred in the Southern and Central Apennines and in the Southern Dinarides-Albanides sector, while only few shocks have affected the Adriatic boundary zones located more to the North (Northern Apennines, Northern Dinarides and Eastern Southern Alps).

Considering this seismicity distribution and the post-seismic relaxation effects that such earthquakes have triggered in the Adria domain [60]-[63], one could suppose that the short-term kinematics of southern Adria may resemble the long-term behaviour, whereas the northern part of Adria, not yet decoupled from the surrounding structures, is moving with a lower rate respect to the long-term one [48] [59]. This differential displacement rate involves a roughly SE-NW compressional regime in the middle Adria zone. It is reasonable to suppose that such transient (or partially transient) shortening phase has systematically developed during the past migration phases of Adria [48] [59]. In the long-term, the total effect of the periodic SE-NW compressional pulses could have caused the formation of the Mid Adriatic Ridge (**Figure 7(d)**), an uplifted structure in the central Adriatic which has been evidenced by seismic surveys and interpreted as a consequence of longitudinal shortening in the Adriatic platform [34] [46] [47].

A number of authors, assuming a rigid behaviour of Adria, have used short-term evidence (geodetic and seismological data) to advance various hypotheses about the configuration and kinematic pattern of one or more

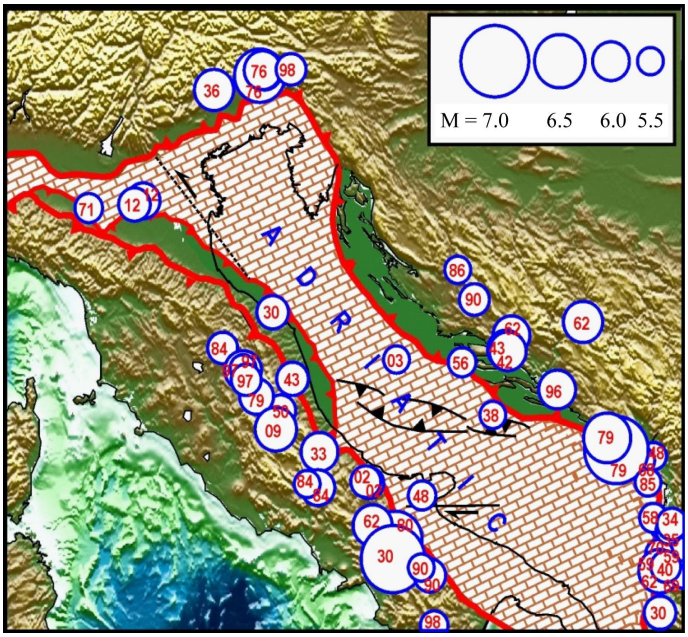

Figure 6. Major earthquakes occurred in the Periadriatic zones since 1930 [48] [49]. Each shock is supposed to allow the decoupling of the Adriatic plate from the surrounding structures.

Adria blocks [17] [35]-[44]. However, as discussed by [46], the expected tectonic implications of the proposed contexts have not properly been compared with the observed Quaternary deformations. In this regard, one should be aware that a reliable recognition of the ongoing plate configuration and kinematics in the study area can only be obtained by an integrated and accurate analysis of the spatio-temporal distribution of major tectonic events, aimed at recognizing the entire evolution of the study area. In fact, a reliable reconstruction of the whole story may impose important constraints on the present tectonic setting, which may considerably help to identify the most reliable interpretation. An attempt in this direction, carried out by [10] [11], taking into account a large amount of long-term data in the whole Mediterranean region, has suggested the evolutionary reconstruction shown in **Figure 7**.

The proposed evolution provides that the Adriatic promontory moved as a part of Africa until the Late Miocene (**Figure 7(a)**). Since that time, the direct contact between the continental Adriatic domain and the buoyant Balkan peninsula (moving roughly westward) caused a profound reorganization of the tectonic kinematic setting in the central Mediterranean area, conditioned by the need of activating less resisted E-W shortening processes (minimum action principle, [10] [11]). This reorganization involved the decoupling of the Adriatic-Ionian and Hyblean plates from Nubia (**Figure 7(b)**), through the activation of the Victor-Hensen and Sicily Channel strike-slip/transtensional fault systems. To accommodate the roughly E-W shortening between the Adria-Ionian plate and the Northwestern Nubia domain (Tunisia), the Hyblean wedge has undergone a roughly NW ward extrusion. On its turn, the indentation of this extruding wedge caused the lateral escape of wedges from the Apennine-Alpine belt (which at that time lain to the east of Sardinia), at the expense of the thinned continental Adriatic and the oceanic Ionian domains (**Figure 7(b)**). The decoupling of the Hyblean wedge from Nubia has been allowed by the activation of the Sicily Channel and the Syracuse fault systems, where post early Messinian deformation is recognized [64] [65].

As argued in detail by Mantovani *et al*. (2009, 2014), the above context can plausibly and coherently account for the complex spatio-temporal distribution of major tectonic events that almost simultaneously started in the Late Miocene and then developed until the upper Pliocene in the central Mediterranean area, such as the formation of the Sicily Channel tectonic zone and the Victor-Hensen fault system, the extensional activity in the central Tyrrhenian basin (Magnaghi-Vavilov), the orogenic pulse that involved the whole Apennine belt, the activation of a major strike-slip discontinuity in the northern Adriatic area (Schio-Vicenza fault system), the roughly northward displacement of the sector of the Maghrebian-Alpine belt which lied north of the Hyblean wedge and

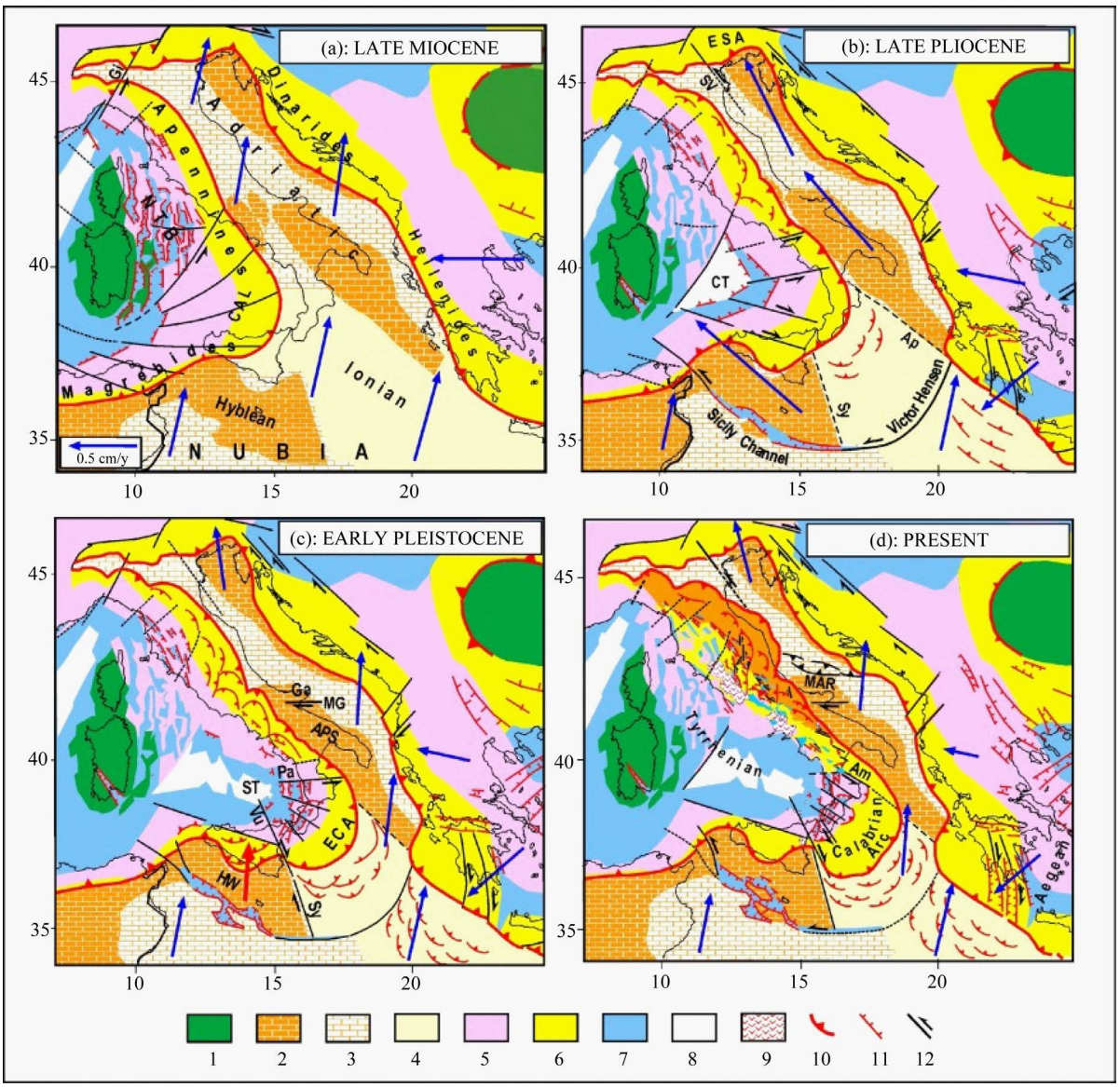

Figure 7. Evolutionary reconstruction of the central Mediterranean region proposed by [10] [11]. (a) Late Miocene. CAL = Calabria, Gi = Giudicarie fault system, NTB = Northern Tyrrhenian basin; (b) Late Pliocene. Ap = Apulian escarpment, CT = Central Tyrrhenian (Magnaghi and Vavilov basins), ESA = Eastern Southern Alps, SV = Schio-Vicenza fault system, Sy = Syracuse escarpment; (c) Early Pleistocene. APS = Apulian Swell, ECA = External Calabrian Arc, Ga = Gargano, HW = Hyblean wedge, MG = Mattinata-Gondola fault, Pa = Palinuro fault, ST = South Tyrrhenian, Sy = Syracuse fault system, Vu = Vulcano fault; (d) Present. Am = Amendolara ridge, MAR = Mid Adriatic Ridge.1) European continental domain; 2, 3) Africa-Adriatic continental and thinned continental domains; 4) Neotethys oceanic domain; 5) Alpine belt; 6) Neogenic accretionary belts; 7, 8) Neogenic extensional basins and oceanized zones; 9) Quaternary magmatism; 10, 11, 12) Major compressional, extensional and transcurrent tectonic features. Thin lines identify the present geographical contours. The paleoposition of the Tunisian coast (thick line) is reported for reference in the evolutionary maps. Blue arrows indicate plate motions with respect to Eurasia [10] [11] [14].

other tectonic events.

Since the late Pliocene (**Figure 7(c)**), due to the entering of thick Adriatic continental lithosphere at the Southern Apennines trench zones, lateral escape of buoyant orogenic wedges mainly developed in the Calabrian sector of the belt. This wedge, stressed by belt-parallel compression has undergone rapid uplift [66] [67] and lateral escape, at the expense of the adjacent Ionian oceanic domain. This process had major effects at both the inner side (opening of the southernmost Tyrrhenian basin, Marsili) and on the outer front (accretionary activity

in the External Calabrian Arc) of the escaping Calabrian wedge. During extrusion, this wedge, laterally bounded by the Palinuro and Vulcano strike-slip guides, has also undergone strong fragmentation, with the formation of several transversal and belt parallel fault systems, in response to belt parallel compression.

During the same evolutionary stage, the southern Adria sector, contemporaneously stressed by the westward push of the Balkan peninsula and the roughly NNE ward push of Nubia (transmitted by the Calabrian Arc), has undergone upward flexure [68] [69]. The fact that only the southern portion of Adria was stressed by the westward push of the Anatolian-Aegean-Balkan system might have induced a dextral shear stress in the central part of that plate, in good correspondence to the Gargano zone, where the Mattinata fault system was reactivated with a dextral movementstill active [70]-[72].

Since the early Pleistocene (**Figure 7(d)**), the direct contact between the northern part of the Calabrian wedge and the thick continental Adria domain caused a significant slowdown of northern Calabria's outward escape, recognized by geological evidence [67], emphasizing the decoupling of the northern sector (slowed down) from the southern one (not slowed down). Furthermore, the orientation of the northern Calabrian escape changed from about ESE to SE ward, as suggested by the available evidence [65].

After the slowdown of northern Calabria, the Palinuro decoupling fault system became almost inactive. However, the outward escape of northern Calabria has not completely ceased, becausein the late Pleistocene the activation of a NW-SE transpressional tectonic zone (Amendolara ridge, **Figure 7(d)** [73]) offshore northern Calabria has allowed such block to maintain some movement towards the Ionian oceanic domain. This extrusion, accompanied by a counterclockwise rotation, could be responsible for the post Middle Pleistocene extensional regime that has occurred in the Crati trough in northern Calabria [67] [74].

Since the late Pleistocene (**Figure 7(d)**), the relative motion of the Adria-Ionian plate with respect to Nubia has undergone a considerable slowdown, due to the increasing resistance to shortening along the surrounding buoyant orogenic structures (Hellenides, Dinarides, Alps and Apennines). This trend suggests that at present the motion of Nubia cannot be significantly different from that of southern Adria.

The proposed reconstruction provides that since the middle Pleistocene the outer sector of the Apennine belt, stressed by Adria, has undergone belt parallel shortening, which has been accommodated by outward extrusion and uplift, as shown with a greater detail in **Figure 8**. The outer mobile portion of the Apennine belt is formed by the Molise-Sannio (MS) wedge in the Southern Apennines, the eastern sector of the Lazio-Abruzzi carbonate platform (ELA) in the Central Apennines, and the Romagna-Marche-Umbria (RMU) and Toscana-Emilia (TE) wedges in the Northern Apennines. The separation of the outer mobile wedges from the inner (Tyrrhenian) sector of the belt has been accommodated by the generation of a series of troughs. The escaping material only includes the sedimentary cover, decoupled from its crustal basement at seismogenic depth (of the order of 6 - 10 km) by mechanically weak lithological horizons, as evidenced by seismic surveys [75]. In particular, a Late Triassic evaporitic layer (Burano formation), forms the base of the Meso-Cenozoic sedimentary cover of most of the extruding wedges. The overall weakness of the Burano formation is related to the presence of evaporite (anydhrite) levels among dolostones [20] [76].

The proposed geodynamic interpretation [10] [12] also suggests that some mobility also characterizes the inner sector of the Apennines, even though such motion develops at lower rates and with a greater northward component with respect to the outer belt (**Figure 8**).

In summary, the proposed evolutionary reconstruction (**Figure 7**) suggests that at present the Adria-Ionian plate is a coherent block (with no significant breaks) moving almost in connection with Nubia. This view and the Nubia-Eurasia relative motion proposed by [4] can reconcile the geodetic velocity field in the southern Adria zone with the absence of a major Adria-Nubia decoupling zone.

3.3. Present Kinematics and Tectonics of the Apennine Belt, Calabrian Arc and Sicily

In the Apennine belt, the GPS kinematic pattern (**Figure 2**) points out a considerable variation of velocity from the outer to the inner sectors. This evidence is illustrated with a greater detail in **Figure 9**, where a tentative identification of roughly homogeneous kinematic domains is shown. The highest velocities (3 - 5 mm/y) and a prevailing NE ward orientation of vectors characterize the outermost belt, including the buried thrusts and folds under the Po Plain, while the lowest velocities (<2 mm/y), with NW ward to Northward orientation, are observed in the innermost belt. These two sectors are separated by an axial zone, characterized by intermediate velocity values and orientations. In the Padanian zone lying north of the buried Apennine folds velocity values

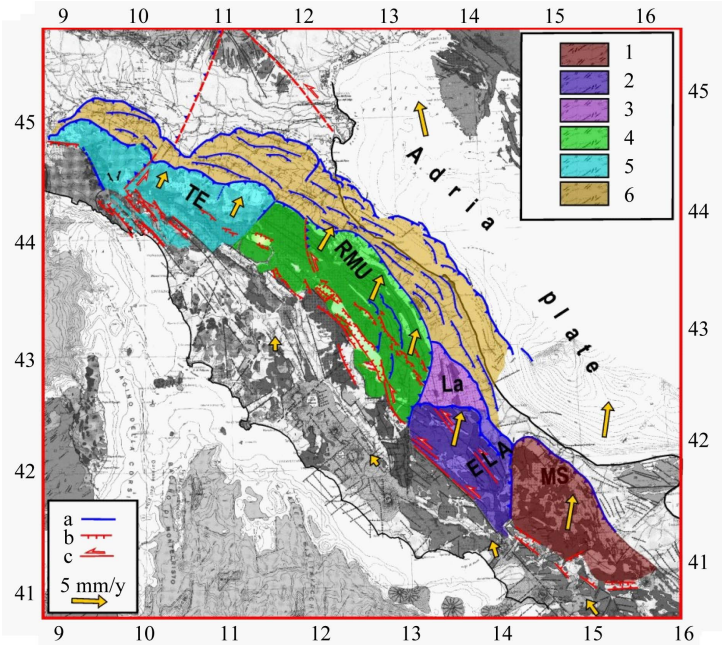

Figure 8. Orogenic wedges that constitute the outer mobile sector of the Apennine belt: 1) Molise-Sannio (MS); 2) Eastern Latium-Abruzzi (ELA); 3) Laga Units (La); 4) Romagna-Marche-Umbria (RMU); 5) Tuscany-Emilia (TE); 6) Outermost buried folds. a, b, c) main compressional, extensional and transcurrent features. Yellow arrows indicate the presumed long term average kinematics of Adria, Apennine wedges and internal zones. Many details about the seismotectonic setting of the Apennine belt are provided by [10]-[12] [14] [49] [58] [59] [76].

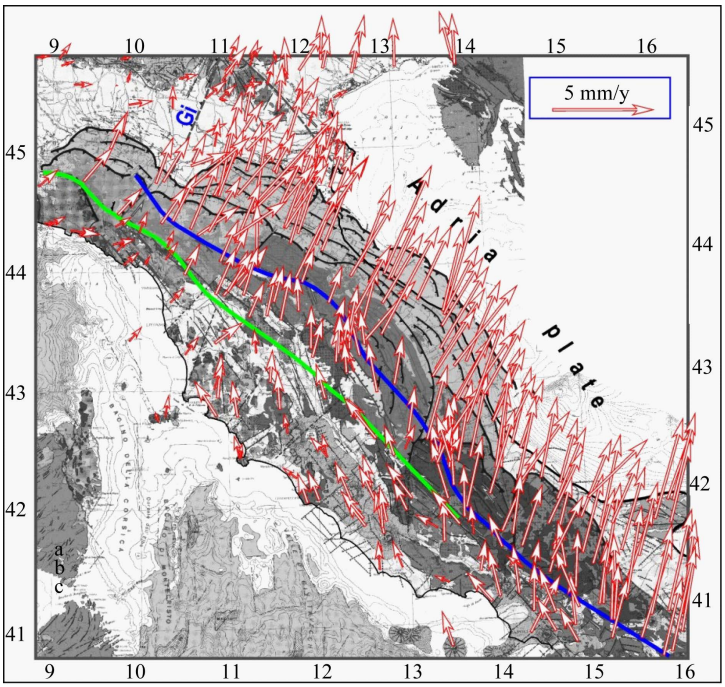

Figure 9. Tentative recognition of the roughly homogeneous kinematic domains in the Apennine belt. See text for comments. Gi = Giudicarie fault system.

show a significant decrease. It can be noted that in the Padanian zone that lies west of the Giudicarie fault system the trends and rates of GPS vectors are significantly different from the ones in the surrounding zones. A discussion about the possible tectonic causes of this evidence is given by [21].

The GPS velocity field given in **Figure 9** is compatible with the kinematic pattern of the Apennine belt deduced by the analysis of long-term evidence [8]-[14] [76] [77], with particular reference to the fact that the outer belt moves significantly faster and with a greater eastward component with respect to the inner belt (**Figure 8**).

The distribution of seismicity (**Figure 10**) in the Apennine belt shows an interesting correspondence between the alignments of major earthquakes and the transition zones from higher to lower geodetic velocities (**Figure 9**).

Other attempts at gaining insights into the present kinematics of the Apennine belt and surroundings by the analysis of geodetic data are reported in literature (see, e.g., the review given by [17]). Some of the considered velocity fields [78] [79] are similar to the one shown in **Figure 2**, but the proposed tectonic interpretations are drastically different from the one described above (**Figure 7(d)** and **Figure 9**), since they mostly invoke the gravitational sinking of the Adriatic subducted lithosphere beneath the Apennine belt as the main driving mechanism of the observed surface kinematics.

However, such view involves some major problems, as argued in the following. Above all, it must be considered that the development of the presumed slab roll-back and consequent trench retreat along the Apennine belt is described with considerable uncertainty in literature. In particular, most authors [80]-[82] suggest that the evidence of subducted lithosphere beneath the Apennine belt is lacking in large sectors of the trench zone. Thus, it is difficult to assume such a discontinuous process as the driving mechanism of the present velocity field in the Apennines, which is characterized by a fairly uniform distribution of rates and orientations all along the belt (**Figure 2**). Furthermore, the above interpretation can hardly explain why the inner Apennine belt has such a different kinematics with respect to the outer belt, as also noted by [17] Nocquet (2012). This last difficulty is also pointed out by the results of numerical modelling, which show that the NE-ward roll-back of the Adriatic plate is expected to induce a similar motion in the upper plate [83], that in this case corresponds to the inner (Tyrrhenian) side of the Apennines.

Other experiments [84] point out that slab roll-back, trench retreat and back arc extension are inhibited when the continental foreland of the subducted lithosphere enters the trench. Since such condition is present along most of the Apennine and Maghrebian trench zones, the plausibility of the slab pull mechanism in those sectors is debatable.

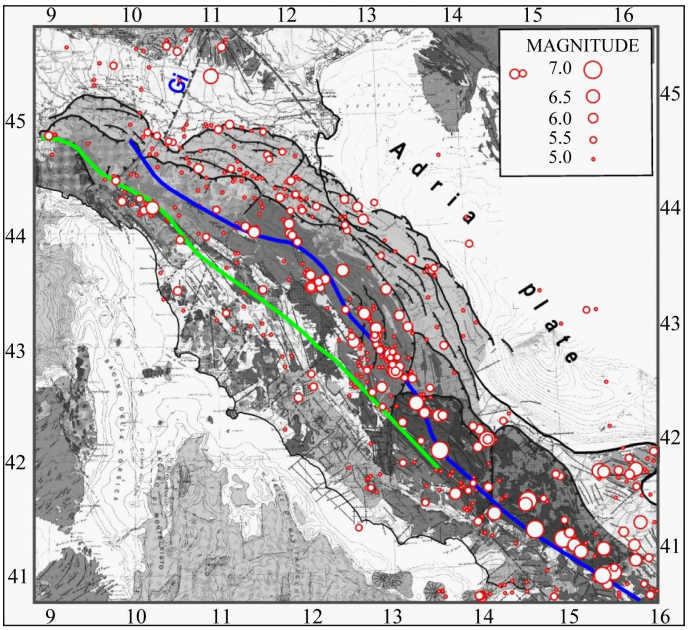

Figure 10. Distribution of major seismicity in the Apennine belt since 1000 A.D. [48]. The coloured lines are taken from **Figure 9**.

Another major problem for the slab roll-back mechanism is explaining some major features of the GPS velocity field in the Calabrian Arc, *i.e*. the only belt sector where the presence of a well-developed slab is clearly documented by the distribution of deep seismicity [64]. In particular one should explain why in Calabria the GPS vectors are almost parallel to the main axis of the belt (**Figure 2**), and in Sicily the vectors are oriented towards the Tyrrhenian basin, *i.e*. about the opposite to what happens in the Apennines. In summary, it seems very difficult to understand why the invoked slab-pull mechanism would induce very different or even opposite effects on the kinematics of the various sectors of the retreating trench zone.

One could rather note that the geodetic velocity field, involving a roughly ENE motion of Calabria and a roughly northward motion of Sicily, is compatible with the present long-term kinematics provided for these two wedges by the proposed evolutionary reconstruction (**Figure 7(d)**). Considering the kinematic/tectonic pattern implied by such reconstruction, the present GPS velocity field in Calabria (**Figure 2**) could be taken as the result of two movements, one induced by the NNE ward motion of Nubia and the other given by a small SE ward motion (1 - 2 mmy) of the Calabrian wedge towards the Ionian domain.

This low value of the Ionian ward motion of Calabria and other evidence have led some authors [7] [42] [43] to suggest that the tectonic mechanism responsible for back arc activity in this sector of the trench is now almost inactive. However, this interpretation is not consistent with the fact that strong seismic activity has occurred in Calabria during the past centuries (1638, M = 7.0 and 6.9; 1783 M = 7.0, 6.6 and 7.0; 1905 M = 7.0; 1908 M = 7.1, [48]), which indicates that southern Calabria is still undergoing strong deformation [67].

A discussion about this problem has been given by [49] [58] [63], who suggest that the recent/present tectonic setting in Calabria may have been influenced by a very rare major tectonic event that has considerably perturbed the strain and stress fields in the central Mediterranean region. It concerns the large westward displacement that the Anatolian-Aegean system underwent in response to the activation of the whole North Anatolian Fault System that was triggered by the very strong earthquake (M = 8) occurred in the easternmost sector of such system in 1939 [85]. In particular it is suggested that such large displacement of the Anatolian-Aegean-Balkan system may have caused a drastic increase of the E-W compressional stress in the northern Ionian and southern Adriatic zones, which might have consequently undergone crustal thickening and upward flexure. Such process may have significantly increased the resistance against the outward extrusion of the Calabrian wedge. This hypothesis could explain why after the post 1939 Anatolia's acceleration seismic activity in Calabria has undergone a considerable reduction [49] [58]. The last strong earthquake in that zone has occurred in 1947 (M = 5.7). The length of the following seismic quiescence (68 years), concerning such seismicity level, is much longer than the average return period of major events (12 years) and of the longest inter-event time (41 years) in that zone [48].

The proposed geodynamic context [10]-[12] provides that the compressional regime induced by the convergence between Nubia (moving roughly NNE ward) and the Anatolian-Aegean system (moving westward) is accommodated by the simultaneous extrusion of the Calabrian wedge (towards the Ionian area) and of the Hyblean wedge (towards North/NNW). Thus, in the ongoing context, one could suppose that the present slowdown of Calabria's escape may emphasize the northward escape of the Hyblean wedge.

In the tectonic context proposed by [10] Mantovani *et al*. (2009) one could expect that at present the probability of strong earthquakes in Calabria is relatively low, whereas such probability may have increased in the decoupling zone between the above two wedges (in particular the Vulcano and Syracuse fault systems, **Figure 7(c)**) and in the northern front of the Hyblean wedge (northern Sicily and southernmost Tyrrhenian basin).

4. Conclusions

The present kinematic pattern of the Italian region, tentatively identified by GPS observations in hundreds of sites, provides significant insights into the geodynamic/tectonic setting in the central Mediterranean area. A significant number of data in the Apulian zone coherently indicate that the southern Adriatic domain moves roughly NE ward. This evidence creates a problem if the Nubia-Eurasia relative motion is taken from global kinematic models, since it implies a significant relative motion between Adria and Nubia, in contrast with the fact that no clear decoupling zone can be recognized between such plates. This major difficulty may be overcome if the alternative Nubia-Eurasia rotation pole proposed by [4] is taken into account. This solution may also account for some primary features of the Quaternary tectonic setting in the whole Mediterranean region.

To explain why the Nubia-Eurasia rotation pole provided by global kinematic models may be not reliable, [4] argue that the plate configuration adopted by such investigation is oversimplified, since it involves a two plates

model (Nubia and Eurasia), notwithstanding that the distribution of seismic and tectonic features in the Mediterranean area suggests the presence of two microplates (Morocco and Iberia, **Figure 1**), not moving in close connection with the Nubia and Eurasia main plates.

It is worth noting that adopting the above four plate configuration the roughly NNE ward Nubia-Eurasia relative motion proposed by [4] can also account, within errors, for the North Atlantic kinematic constraints considered for the definition of the global kinematic models.

The GPS velocity field (**Figure 2**) clearly defines the kinematics of two Adriatic zones, one located in the southern part (Apulia) and the other located in the northernmost Adria domain (Venetian plain). If such kinematic constraints are interpreted as related to a rigid structure, the resulting Adria-Eurasia rotation pole is located in the Western Alps. Similar results have been obtained by the inversion of earthquake slip vectors in Periadriatic zones. This short-term solution would imply an independent motion between Nubia and Adria, whatever Nubia-Eurasia Euler pole is adopted, among the ones so far proposed. Since this result can hardly be reconciled with the lack of a decoupling zone between Nubia and Adria, we suppose that such evidence might result from a transient non-rigid behavior of the Adria plate. This hypothesis is supported by the fact that in the last tens of years (since 1930) most major Periadriatic earthquakes have occurred in the southern boundary zones (Northern Hellenides, Albanides, Southern Dinarides, Southern and Central Apennines). Such distribution of decoupling fault slips implies that at present the southern part of Adria can move in line with its long term behaviour, whereas the mobility of the northern Adria sector is still limited by the fact that in the last tens of years, the decoupling seismic zones in the Northern Dinarides, Eastern Southern Alps and Northern Apennines have not undergone significantactivations. This differential short-term behaviours would imply the development of a transient phase of internal deformation in the Adria plate. This effect, systematically developed during the analogous transient compressional phases occurred in the past evolution, could account for the presence in the central Adriatic area of the Mid Adriatic ridge, an uplifted structure explained as a consequence of longitudinal compression in the Adria domain.

The geodetic field in the Apennine belt, characterized by fairly different kinematic patterns in the inner and outer sectors of the belt, is compatible with the long term kinematic pattern deduced by the analysis of the Pliocene-Quaternary deformation pattern in the central Mediterranean region [8] [10] [12] [14], whereas it can hardly be reconciled with the implications of the main alternative geodynamic mechanism often mentioned in literature, invoking the contribution of slab roll-back at the Adriatic-Apennine trench zone.

In the Calabrian Arc and Sicily the geodetic field is compatible with the hypothesis that, in response to the convergence of the confining plates (Nubia, Eurasia and the Anatolian-Aegean system), the Calabrian and Hyblean wedges are undergoing lateral escape, involving a roughly ENE ward motion for Calabria and a roughly Northward motion for the Hyblean block. At present, the second process is developing at higher rates with respect to the first one, due to the effects of the post 1939 large westward displacement of the Anatolian-Aegean system [49] [58].

Acknowledgements

We thank two anonymous reviewers for their constructive comments.

References

[1] DeMets, C., Gordon, R.G. and Argus, D.F. (2010) Geologically Current Plate Motions. *Geophysical Journal International*, **181**, 1-80. http://dx.doi.org/10.1111/j.1365-246X.2009.04491.x

[2] Argus, D.F., Gordon, R.G., Heflin, M.B., Ma, C., Eanes, R.J., Willis, P., Peltier, W.R. and Owen, S.E. (2010) The Angular Velocities of the Plates and the Velocity of Earth's Centre from Space Geodesy. *Geophysical Journal International*, **180**, 913-960. http://dx.doi.org/10.1111/j.1365-246X.2009.04463.x

[3] Altamimi, Z., Métivier, L. and Collilieux, X. (2012) ITRF2008 Plate Motion Model. *Journal of Geophysical Research*, **117**, B07402. http://dx.doi.org/10.1029/2011JB008930

[4] Mantovani, E., Viti, M., Babbucci, D. and Albarello, D. (2007)Nubia-Eurasia Kinematics: an Alternative Interpretation from Mediterranean and North Atlantic Evidence. *Annals of Geophysics*, **50**, 311-336.

[5] Malinverno, A. and Ryan, W.B.F. (1986) Extension in the Tyrrhenian Sea and Shortening in the Apennines as Result of Arc Migration Driven by Sinking of the Lithosphere. *Tectonics*, **5**, 227-245. http://dx.doi.org/10.1029/TC005i002p00227

[6] Schellart, W.P. and Lister, G.S. (2004) Tectonic Models for the Formation of Arc-Shaped Convergent Zones and Backarc Basins. *The Geological Society of America Special Paper*, **383**, 237-258. http://dx.doi.org/10.1130/0-8137-2383-3(2004)383[237:tmftfo]2.0.co;2

[7] Faccenna, C., Funiciello, F., Civetta, L., D'Antonio, M., Moroni, M. and Piromallo, C. (2007) Slab Disruption, Mantle Circulation, and the Opening of the Tyrrhenian Basins. *The Geological Society of America Special Paper*, **418**, 153-169. http://dx.doi.org/10.1130/2007.2418(08)

[8] Mantovani, E., Babbucci, D., Viti, M., Albarello, D., Mugnaioli, E., Cenni, N. and Casula, G. (2006) Post-Late Miocene Kinematics of the Adria Microplate: Inferences from Geological, Geophysical and Geodetic data. In: Pinter, N., Grenerczy, G., Weber, J., Stein, S. and Medak, D., Eds., *The Adria Microplate*: *GPS Geodesy, Tectonics and Hazard*, Vol. 61, NATO Science Series IV-Earth and Environmental Sciences, Springer, 51-69. http://dx.doi.org/10.1007/1-4020-4235-3_04

[9] Mantovani, E., Viti, M., Babbucci, D. and Tamburelli, C. (2007) Major Evidence on the Driving Mechanism of the Tyrrhenian Apennines Trench-Arc Back Arc System from CROP Seismic Data. *Bollettino Della Societa Geologica Italiana*, **126**, 459-471.

[10] Mantovani, E., Babbucci, D., Tamburelli, C. and Viti, M. (2009) A Review on the Driving Mechanism of the Tyrrhenian-Apennines system: Implications for the Present Seismotectonic Setting in the Central-Northern Apennines. *Tectonophysics*, **476**, 22-40. http://dx.doi.org/10.1016/j.tecto.2008.10.032

[11] Mantovani, E., Viti, M., Babbucci, D., Tamburelli, C., Cenni, N., Baglione, M. and D'Intinosante, V. (2014) Generation of Back-Arc Basins as Side Effect of Shortening Processes: Examples from the Central Mediterranean. *International Journal of Geosciences*, **5**, 1062-1079. http://dx.doi.org/10.4236/ijg.2014.510091

[12] Viti, M., Mantovani, E., Babbucci, D. and Tamburelli, C. (2006) Quaternary Geodynamics and Deformation Pattern in the Southern Apennines: Implications for Seismic Activity. *Bollettino Della Societa Geologica Italiana*, **125**, 273-291.

[13] Viti, M., Mantovani, E., Babbucci, D. and Tamburelli, C. (2009) Generation of Trench-Arc-Back-Arc Systems in the Western Mediterranean Region Driven by Plate Convergence. *Bollettino Della Societa Geologica Italiana*, **128**, 89-106.

[14] Viti, M., Mantovani, E., Babbucci, D. and Tamburelli, C. (2011) Plate Kinematics and Geodynamics in the Central Mediterranean. *Journal of Geodynamics*, **51**, 190-204. http://dx.doi.org/10.1016/j.jog.2010.02.006

[15] DeMets, C., Gordon, R.G., Argus, D.F. and Stein, S. (1990) Current Plate Motions. *Geophysical Journal International*, **101**, 425-478. http://dx.doi.org/10.1111/j.1365-246X.1990.tb06579.x

[16] DeMets, C., Gordon, R.G., Argus, D.F. and Stein, S. (1994) Effect of Recent Revisions to the Geomagnetic Reversal Time Scale on Estimates of Current Plate Motions. *Geophysical Research Letters*, **21**, 2191-2194. http://dx.doi.org/10.1029/94GL02118

[17] Nocquet, J.-M. (2012) Present-Day Kinematics of the Mediterranean: A Comprehensive Overview of GPS Results. *Tectonophysics*, **579**, 220-242. http://dx.doi.org/10.1016/j.tecto.2012.03.037

[18] Herring, T.A., King, R.W. and McClusky, S.C. (2010) GAMIT Reference Manual, GPS Analysis at MIT, Release 10.4. Department of Earth, Atmospheric and Planetary Sciences, Massachusetts Institute of Technology, Cambridge, USA.

[19] Dong, D., Herring, T.A. and King, R.W. (1998) Estimating Regional Deformation from a Combination of Space and Terrestrial Geodetic Data. *Journal of Geodesy*, **72**, 200-214. http://dx.doi.org/10.1007/s001900050161

[20] Cenni, N., Mantovani, E., Baldi, P. and Viti, M. (2012) Present Kinematics of Central and Northern Italy from Continuous GPS Measurements. *Journal of Geodynamics*, **58**, 62-72. http://dx.doi.org/10.1016/j.jog.2012.02.004

[21] Cenni, N., Viti, M., Baldi, P., Mantovani, E., Bacchetti, M. and Vannucchi, A. (2013) Present Vertical Movements in Central and Northern Italy from GPS Data: Possible Role of Natural and Anthropogenic Causes. *Journal of Geodynamics*, **71**, 74-85. http://dx.doi.org/10.1016/j.jog.2013.07.004

[22] Herring, T.A., King, R.W. and McClusky, S.C. (2010) Global Kalman Filter VLBI and GPS Analysis Program, GLOBK Reference Manual, Release 10.4. Department of Earth, Atmospheric and Planetary Sciences, Massachusetts Institute of Technology, Cambridge, USA.

[23] Blewitt, G. and Lavallée, D. (2002) Effect of Annual Signals on Geodetic Velocity. *Journal of Geophysical Research*, **107**, 2145. http://dx.doi.org/10.1029/2001JB000570

[24] Bos, M.S., Fernandes, R.M.S., Williams, S.D.P. and Bastos, L. (2008) Fast Error Analysis of Continuous GPS Observations. *Journal of Geodesy*, **82**, 157-166. http://dx.doi.org/10.1007/s00190-007-0165-x

[25] Bos, M.S., Bastos, L. and Fernandes, R.M.S. (2010) The Influence of Seasonal Signals on the Estimation of the Tectonic Motion in Short Continuous GPS Time-Series. *Journal of Geodynamics*, **49**, 205-209. http://dx.doi.org/10.1016/j.jog.2009.10.005

[26] Hackl, M., Malservisi, R., Hugentobler, U. and Wonnacott, R. (2011) Estimation of Velocity Uncertainties from GPS

Time Series: Examples from the Analysis of the South African TrigNet Network. *Journal of Geophysical Research*, **116**, B11404. http://dx.doi.org/10.1029/2010jb008142

[27] Santamaría-Gómez, A., Bouin, M.N., Collilieux, X. and Wöppelmann, G. (2011) Correlated Errors in GPS Position Time Series: Implications for Velocity Estimates. *Journal of Geophysical Research*, **116**, B01405. http://dx.doi.org/10.1029/2010jb007701

[28] Williams, S.D.P., Bock, Y., Fang, P., Jamason, P., Nikolaidis, R-M., Prawirodirdjo, L., Miller, M. and Johnson, J. (2004) Error Analysis of Continuous GPS Position Time Series. *Journal of Geophysical Research*, **109**, B03412. http://dx.doi.org/10.1029/2003jb002741

[29] Williams, S.D.P. (2008) CATS: GPS Coordinate Time Series Analysis Software. *GPS Solutions*, **12**, 147-153. http://dx.doi.org/10.1007/s10291-007-0086-4

[30] Bos, M.S., Fernandes, R.M.S., Williams, S.D.P. and Bastos, L. (2013) Fast Error Analysis of Continuous GNSS Observations with Missing Data. *Journal of Geodesy*, **87**, 351-360. http://dx.doi.org/10.1007/s00190-012-0605-0

[31] Nicolai, C. and Gambini, R. (2007) Structural Architecture of the Adria Platform-and-Basin System. *Bollettino Della Societa Geologica Italiana* (*Italian Journal of Geosciences*), Special Issue **7**, 21-37.

[32] Fantoni, R. and Franciosi, R. (2010) Tectono-sedimentary Setting of the Po Plain and Adriatic Foreland. *Rendiconti Lincei - Scienze Fisiche e Naturali*, **21**, S197-S209. http://dx.doi.org/10.1007/s12210-010-0102-4

[33] Anderson, H. and Jackson, J. (1987) Active Tectonics of the Adriatic Region. *Geophysical Journal International*, **91**, 937-983. http://dx.doi.org/10.1111/j.1365-246X.1987.tb01675.x

[34] Scisciani, V. and Calamita, F. (2009) Active Intraplate Deformation within Adria: Examples from the Adriatic Region. *Tectonophysics*, **476**, 57-72. http://dx.doi.org/10.1016/j.tecto.2008.10.030

[35] Weber, J., Vrabec, M., Pavlovčič-Prešeren, P., Dixon, T., Jiang, Y. and Stopar, B. (2010) GPS-Derived Motion of the Adriatic Microplate from Istria Peninsula and Po Plain Sites, and Geodynamic Implications. *Tectonophysics*, **483**, 214-222. http://dx.doi.org/10.1016/j.tecto.2009.09.001

[36] Westaway, R. (1990) Present-Day Kinematics of the Plate Boundary Zone between Africa and Europe, from the Azores to the Aegean. *Earth and Planetary Science Letters*, **96**, 393-406. http://dx.doi.org/10.1016/0012-821X(90)90015-P

[37] Console, R., Di Giovambattista, R., Favali, P., Presgrave, B.W. and Smriglio, G. (1993) Seismicity of the Adriatic Microplate. *Tectonophysics*, **218**, 343-354. http://dx.doi.org/10.1016/0040-1951(93)90323-C

[38] Favali, P., Funiciello, R., Mattietti, G., Mele, G. and Salvini, F. (1993) An Active Margin Across the Adriatic Sea (Central Mediterranean Sea). *Tectonophysics*, **219**, 109-117. http://dx.doi.org/10.1016/0040-1951(93)90290-Z

[39] Meletti, C., Patacca, E. and Scandone, P. (2000) Construction of a Seismotectonic Model: The Case of Italy. *Pure and Applied Geophysics*, **157**, 11-35. http://dx.doi.org/10.1007/PL00001089

[40] Oldow, J.S., Ferranti, L., Lewis, D.S., Campbell, J.K., D'Argenio, B., Catalano, R., Pappone, G., Carmignani, L., Conti, P. and Aiken, C.L.V. (2002) Active Fragmentation of Adria, the North African Promontory, Central Mediterranean Orogeny. *The Geological Society of America*, **9**, 779-782.

[41] Battaglia, M., Murray, M.H., Serpelloni, E. and Burgmann, R. (2004) The Adriatic Region: An Independent Microplate within the Africa-Eurasia Collision Zone. *Geophysical Research Letters*, **31**, L09605. http://dx.doi.org/10.1029/2004gl019723

[42] Goes, S., Giardini, D., Jenny, S., Hollenstein, C., Kahle, H.G. and Geiger, A. (2004) A Recent Tectonic Reorganization in the South-Central Mediterranean. *Earth and Planetary Science Letters*, **225**, 335-345. http://dx.doi.org/10.1016/j.epsl.2004.07.038

[43] Serpelloni, E., Anzidei, M., Baldi, P., Casula, G. and Galvani, G. (2005) Crustal Velocity and Strain-Rate Fields in Italy and Surrounding Regions: New Results from the Analysis of Permanent and Non-Permanent GPS Networks. *Geophysical Journal International*, **161**, 861-880. http://dx.doi.org/10.1111/j.1365-246X.2005.02618.x

[44] D'Agostino, N., Avallone, A., Cheloni, D., D'Anastasio, E., Mantenuto, S. and Selvaggi, G. (2008) Active Tectonics of the Adriatic Region from GPS and Earthquake Slip Vectors. *Journal of Geophysical Research*, **113**, B12413. http://dx.doi.org/10.1029/2008jb005860

[45] Babbucci, D., Tamburelli, C., Viti, M., Mantovani, E., Albarello, D., D'Onza, F., Cenni, N. and Mugnaioli, E. (2004) Relative Motion of the Adriatic with Respect to the Confining Plates: Seismological and Geodetic Constraints. *Geophysical Journal International*, **159**, 765-775. http://dx.doi.org/10.1111/j.1365-246X.2004.02403.x

[46] Argnani, A. (2006). Some Issues regarding the Central Mediterranean Neotectonics. *Bollettino di Geofisica Teorica ed Applicata*, **47**, 13-37.

[47] Finetti, I.R. and Del Ben, A. (2005) Crustal Tectono-stratigraphic Setting of the Adriatic Sea from new CROP Seismic Data. In: Finetti, I.R., Ed., *Deep Seismic Exploration of the Central Mediterranean and Italy, CROP PROJECT*. El-

sevier, Amsterdam, 519-548 (Chapter 23).

[48] Rovida, A., Camassi, R., Gasperini, P. and Stucchi, M., Eds. (2011) CPTI11, the 2011 Version of the Parametric Catalogue of Italian Earthquakes. Milano, Bologna. http://emidius.mi.ingv.it/CPTI

[49] Viti, M., Mantovani, E., Babbucci, D., Cenni, N. and Tamburelli, C. (2015) Where the Next Strong Earthquake in the Italian Peninsula? Insights by a Deterministic Approach. *Bollettino di Geofisica Teorica ed Applicata*, **56**, 329-350.

[50] Alasset, P.J. and Meghraoui, M. (2005) Active Faulting in the Western Pyrenees (France): Paleoseismic Evidence for Late Holocene Ruptures. *Tectonophysics*, **409**, 39-54. http://dx.doi.org/10.1016/j.tecto.2005.08.019

[51] Lacan, P. and Ortuno, M. (2012) Active Tectonics of Pyrenees: A Review. *Journal of Iberian Geology*, **38**, 9-30.

[52] Villamor, P., Capote, R., Stirling, M.W., Tsige, M., Berryman, K.R., Martínez-Díaz, J.J. and Martín-González, F. (2012) Contribution of Active Faults in the Intraplate Area of Iberia to Seismic Hazard: The Alentejo-Plasencia Fault. *Journal of Iberian Geology*, **38**, 85-111. http://dx.doi.org/10.5209/rev_jige.2012.v38.n1.39207

[53] Roest, W.R. and Srivastava, S.P. (1991) Kinematics of the Plate Boundaries between Eurasia, Iberia, and Africa in the North Atlantic from the Late Cretaceous to the Present. *Geology*, **19**, 613-616. http://dx.doi.org/10.1130/0091-7613(1991)019<0613:KOTPBB>2.3.CO;2

[54] Anguita, F. and Hernan, F. (2000) The Canary Islands: AUnifying Model. *Journal of Volcanology and Geothermal Research*, **103**, 1-26. http://dx.doi.org/10.1016/S0377-0273(00)00195-5

[55] Geyer, A. and Martí, J. (2010) The Distribution of Basaltic Volcanism on Tenerife, Canary Islands: Implications on the Origin and Dynamics of the Rift Systems. *Tectonophysics*, **483**, 310-326. http://dx.doi.org/10.1016/j.tecto.2009.11.002

[56] Martì, J., Pinel, V., Lopez, C., Geyer, A., Abella, R., Tarraga, M., Blanco, M.J., Castro, A. and Rodrıguez, C. (2013) Causes and Mechanisms of the 2011-2012 El Hierro (Canary Islands) Submarine Eruption. *Journal of Geophysical Research*: *Solid Earth*, **118**, 823-839. http://dx.doi.org/10.1002/jgrb.50087

[57] Saria, E., Calais, E., Altamimi, Z., Willis, P. and Farah, H. (2013) A New Velocity Field for Africa from Combined GPS and DORIS Space Geodetic Solutions: Contribution to the Definition of the African Reference Frame (AFREF). *Journal of Geophysical Research*: *Solid Earth*, **118**, 1677-1697. http://dx.doi.org/10.1002/jgrb.50137

[58] Mantovani, E., Viti, M., Babbucci, D., Tamburelli, C., Cenni, N., Baglione, M. and D'Intinosante, V. (2015) Recognition of PeriAdriatic Seismic Zones Most Prone to Next Major Earthquakes: Insights from a Deterministic Approach. In: D'Amico, S., Ed., *Earthquakes and Their Impact on Society*. Springer Natural Hazard Series, Springer, 43-80.

[59] Mantovani, E., Viti, M., Babbucci, D., Tamburelli, C., Cenni, N., Baglione, M. and D'Intinosante,V. (2015) Present Tectonic Setting and Spatio-Temporal Distribution of Seismicity in the Apennine Belt. *International Journal of Geosciences*, **6**, 429-454. http://dx.doi.org/10.4236/ijg.2015.64034

[60] Viti, M., D'Onza, F., Mantovani, E., Albarello, D. and Cenni, N. (2003) Post-seismic Relaxation and Earthquake Triggering in the Southern Adriatic Region. *Geophysical Journal International*, **153**, 645-657. http://dx.doi.org/10.1046/j.1365-246X.2003.01939.x

[61] Viti, M., Mantovani, E., Cenni, N. and Vannucchi, A. (2012) Post-Seismic Relaxation: An Example of Earthquake Triggering in the Apennine Belt (1915-1920). *Journal of Geodynamics*, **61**, 57-67. http://dx.doi.org/10.1016/j.jog.2012.07.002

[62] Viti, M., Mantovani, E., Cenni, N. and Vannucchi, A. (2013) Interaction of Seismic Sources in the Apennine Belt. *Physics and Chemistry of the Earth*, **63**, 25-35. http://dx.doi.org/10.1016/j.pce.2013.03.005

[63] Mantovani, E., Viti, M., Babbucci, D., Cenni, N., Tamburelli, C. and Vannucchi, A. (2012) Middle Term Prediction of Earthquakes in Italy: Some Remarks on Empirical and Deterministic Approaches. *Bollettino di Geofisica Teorica ed Applicata*, **53**, 89-111.

[64] Finetti, I.R. (2005) The Calabrian Arc and Subducting Ionian Slab from New CROP Seismic Data. In: Finetti, I.R., Ed., *Deep Seismic Exploration of the Central Mediterranean and Italy*, *CROP PROJECT*. Elsevier, Amsterdam, 393-412 (Chapter 17).

[65] Del Ben, A., Barnaba, C. and Taboga, A. (2008) Strike-slip Systems as the Main Tectonic Features in the Plio-Quaternary Kinematics of the Calabrian Arc. *Marine Geophysical Researches*, **29**, 1-12. http://dx.doi.org/10.1007/s11001-007-9041-6

[66] Westaway, R. (1993) Quaternary Uplift of Southern Italy. *Journal of Geophysical Research*, **98**, 741-772. http://dx.doi.org/10.1029/93JB01566

[67] Zecchin, M., Praeg, D., Ceramicola, S. and Muto, F. (2015) Onshore to Offshore Correlation of Regional Unconformities in the Plio-Pleistocene Sedimentary Successions of the Calabrian Arc (Central Mediterranean). *Earth-Science Reviews*, **142**, 60-78. http://dx.doi.org/10.1016/j.earscirev.2015.01.006

[68] Moretti, I. and Royden, L. (1988) Deflection, Gravity Anomalies and Tectonics of Doubly Subducted Continental Lithosphere: Adriatic and Ionian Seas. *Tectonics*, **7**, 875-893. http://dx.doi.org/10.1029/TC007i004p00875

[69] Argnani, A., Frugoni, F., Cosi, R., Ligi, M. and Favali, P. (2001) Tectonics and Seismicity of the Apulian Ridge South of Salento Peninsula (Southern Italy). *Annals of Geophysics*, **44**, 527-540.

[70] Chilovi, C., De Feyter, J. and Pompucci, A. (2000) Wrench Zone Reactivation in the Adriatic Block: The Example of the Mattinata Fault System (SE Italy). *Bollettino Della Societa Geologica Italiana*, **119**, 3-8.

[71] Di Bucci, D. and Mazzoli, S. (2003) The October-November 2002 Molise Seismic Sequence (Southern Italy): An Expression of Adria Intraplate Deformation. *The Geological Society of London*, **160**, 503-506. http://dx.doi.org/10.1144/0016-764902-152

[72] Tondi, E., Piccardi, L., Cacon, S., Kontny, B. and Cello, G. (2005) Structural and Time Constraints for Dextral Shear Along the Seismogenic Mattinata Fault (Gargano, Southern Italy). *Journal of Geodynamics*, **40**, 134-152. http://dx.doi.org/10.1016/j.jog.2005.07.003

[73] Ferranti, L., Burrato, P., Pepe, F., Santoro, E., Mazzella, M.E., Morelli, D., Passaro, S. and Vannucci, G. (2014) An Active Oblique Contractional Belt at the Transition Between the Southern Apennines and Calabrian Arc: The Amendolara Ridge, Ionian Sea, Italy. *Tectonics*, **33**, 2169-2194. http://dx.doi.org/10.1002/2014TC003624

[74] Tansi, C, Iovine, G. and Folino Gallo, M. (2005) Tettonica Attiva e Recente, e Manifestazioni Gravitative Profonde, Lungo il Bordo Orientale del Graben del Fiume Crati (Calabria Settentrionale). *Bollettino Della Societa Geologica Italiana*, **124**, 563-578.

[75] Mirabella, F., Barchi, M., Lupattelli, A., Stucchi, E. and Ciaccio, M.G. (2008) Insights on the Seismogenic Layer Thickness from the Upper Crust Structure of the Umbria-Marche Apennines (Central Italy). *Tectonics*, **27**, TC1010. http://dx.doi.org/10.1029/2007TC002134

[76] Mantovani, E., Viti, M., Cenni, N., Babbucci, D., Tamburelli, C., Baglione, M. and D'Intinosante, V. (2015) Seismotectonics and Present Seismic Hazard in the Tuscany-Romagna-Marche-Umbria Apennines (Italy). *Journal of Geodynamics*, **89**, 1-14. http://dx.doi.org/10.1016/j.jog.2015.05.001

[77] Viti, M., Mantovani, E., Babbucci, D., Tamburelli, C., Cenni, N., Baglione, M. and D'Intinosante, V. (2015) Belt-Parallel Shortening in the Northern Apennines and Seismotectonic Implications. *International Journal of Geosciences*, **6**, 938-961. http://dx.doi.org/10.4236/ijg.2015.68075

[78] Bennett, R.A., Serpelloni, E., Hreinsdóttir, S., Brandon, M.T., Buble, G., Basic., T., Casale, G., Cavaliere, A., Anzidei, M., Marjonovic, M., Minelli, G., Molli, G. and Montanari, A. (2012) Syn-Convergent Extension Observed Using the RETREAT GPS Network, Northern Apennines, Italy. *Journal of Geophysical Research*, **117**, B04408. http://dx.doi.org/10.1029/2011jb008744

[79] Devoti, R., Esposito, A., Pietrantonio, G., Pisani, A.R. and Riguzzi, F. (2011) Evidence of Large Scale Deformation Patterns from GPS data in the Italian Subduction Boundary. *Earth and Planetary Science Letters*, **311**, 230-241. http://dx.doi.org/10.1016/j.epsl.2011.09.034

[80] Spakman, W. and Wortel, R. (2004) A Tomographic View on Western Mediterranean Geodynamics. In: Cavazza, W., Roure, F., Spakman, W., Stampfli, G.M. and Ziegler, P., Eds., *The TRANSMED Atlas, The Mediterranean Region from Crust to Mantle*, 31-52. http://dx.doi.org/10.1007/978-3-642-18919-7_2

[81] Lucente, F.P., Margheriti, L., Piromallo, C. and Barruol, G. (2006) Seismic Anisotropy Reveals the Long Route of the Slab Through the Western-Central Mediterranean Mantle. *Earth and Planetary Science Letters*, **41**, 517-529. http://dx.doi.org/10.1016/j.epsl.2005.10.041

[82] Scafidi, D. and Solarino, S. (2012) Can Local Earthquake Tomography Settle the Matter About Subduction in the Northern and Central Apennines? Response from a New High Resolution P Velocity and Vp/Vs Ratio 3-D Model. *Tectonophysics*, **554-557**, 63-73. http://dx.doi.org/10.1016/j.tecto.2012.06.007

[83] Schellart, W.P. and Moresi, L. (2013) A New Driving Mechanism for Backarc Extension and Backarc Shortening Through Slab Sinking Induced Toroidal And Poloidal Mantle Flow: Results from Dynamic Subduction Models with an Overriding Plate. *Journal of Geophysical Research*: *Solid Earth*, **118**, 3221-3248. http://dx.doi.org/10.1002/jgrb.50173

[84] Magni, V., Van Hunen, J., Funiciello, F. and Faccenna, C. (2012) Numerical Models of Slab Migration in Continental Collision Zones. *Solid Earth*, **3**, 293-306. http://dx.doi.org/10.5194/se-3-293-2012

[85] Barka, A.A. (1996) Slip Distribution along the North Anatolian Fault Associated with the Large Earthquakes of the Period 1939 to 1967. *Bulletin of the Seismological Society of America*, **86**, 1238-1254.

Appendix. Velocities of the GPS sites considered in this study in the ITRF2008 reference frame [3]. N = number of effective observation days. T = observation time interval. Lon, Lat and H = station coordinates (longitude ˚E, latitude ˚N and height above the sea level). V_N and σV_N, V_E and σV_E, V_H and σV_H = North, East and Vertical components of the site velocity and related uncertainties (in mm/yr). The methodology adopted for the analysis of geodetic measurements is described by [20]-[21].

Code	N	T (yr)	Lon.	Lat.	H (m)	V_N	σV_N	V_E	σV_E	V_H	σV_H
ACCA	2707	8.19	15.331	41.159	716.184	19.4	0.2	23.8	0.2	1.0	0.5
ACCE	1870	5.69	6.988	44.476	1321.749	15.9	0.3	20.9	0.3	0.8	1.2
ACER	2565	8.02	15.942	40.787	764.673	19.7	0.1	23.3	0.1	0.2	0.4
ACOM	4074	12.03	13.515	46.548	1774.675	16.7	0.1	21.3	0.1	1.0	0.4
AFAL	3818	12.07	12.175	46.527	2284.080	16.2	0.1	20.5	0.2	1.9	0.3
AGNE	2143	7.24	7.140	45.468	2354.613	15.9	0.4	20.6	0.4	0.9	1.0
ALAT	1911	6.32	13.384	41.673	286.625	17.6	0.5	21.6	0.2	0.4	0.8
ALBI	1139	3.19	16.456	39.946	967.556	20.8	1.4	22.6	0.7	0.8	2.1
ALIF	1948	6.26	14.335	41.327	167.661	17.3	0.4	22.3	0.4	−1.9	1.3
ALIN	1749	5.58	8.616	44.923	146.013	16.6	0.2	20.3	0.2	−1.0	0.8
ALRA	2279	8.44	14.034	41.734	969.786	19.4	0.5	23.6	0.6	1.1	1.3
ALSN	1499	4.40	8.616	44.923	146.666	16.5	0.2	20.5	0.2	−1.2	0.7
ALTA	1285	4.13	16.559	40.823	537.773	19.9	0.2	23.9	0.2	−0.4	0.7
AMAN	933	3.08	16.077	39.120	58.864	19.2	0.5	23.4	0.5	1.2	1.6
AMPE	2322	6.94	12.799	46.415	616.471	16.9	0.2	21.5	0.2	1.6	0.8
AMUR	2988	8.93	16.604	40.907	549.439	19.8	0.1	23.6	0.1	0.1	0.2
ANCG	4072	9.22	13.502	43.603	109.808	19.5	0.2	22.4	0.1	0.9	0.5
ANCN	1412	3.96	13.532	43.607	213.879	20.5	0.4	23.1	0.3	0.2	0.6
ANGE	1856	7.04	15.184	40.931	921.237	18.5	0.2	22.3	0.2	0.5	0.7
AO01	1855	6.51	7.321	45.737	659.784	15.9	0.3	20.3	0.2	1.7	0.8
AOST	802	3.52	7.345	45.741	624.089	15.7	1.3	20.9	0.8	0.8	2.8
APRI	2281	7.23	12.665	41.597	125.090	15.9	0.2	21.5	0.2	0.1	0.7
AQRA	2587	9.07	13.374	42.366	747.263	17.2	0.2	21.0	0.3	−1.1	0.8
AQSA	715	2.90	16.084	39.721	881.751	18.5	0.8	23.0	0.9	1.1	2.5
AQUI	4853	14.55	13.350	42.368	713.072	17.7	0.1	22.0	0.1	−0.4	0.2
AQUM	1370	4.02	13.467	42.328	640.549	17.3	0.4	21.9	0.4	−2.8	1.0
ARBU	1431	5.66	8.594	39.525	312.786	17.7	0.5	22.1	0.6	−2.0	2.4
ARCA	2213	7.05	16.226	39.367	279.696	19.0	0.2	24.0	0.2	−0.5	0.7
ASCC	1852	6.63	13.593	42.857	206.598	18.5	0.2	23.3	0.2	0.4	1.0
ASCG	736	3.52	13.606	42.852	188.049	19.9	0.8	24.1	0.8	−0.9	2.5
ASIA	1992	6.90	11.525	45.866	1093.680	16.5	0.5	21.4	0.5	−2.0	2.2
ASTI	1529	5.29	8.203	44.906	207.045	16.6	0.4	19.9	0.5	0.1	1.5
ATBU	1793	5.22	12.548	43.476	1046.290	18.8	0.2	22.0	0.3	0.6	0.7

Continued

ATFO	1412	6.03	12.567	43.370	1020.427	18.4	0.3	23.7	0.4	2.0	0.9
ATLO	1839	5.32	12.407	43.315	652.486	17.4	0.2	21.1	0.2	0.4	0.6
ATMI	1091	3.48	12.267	43.334	573.059	16.5	0.7	22.4	0.7	3.3	1.9
ATTE	1875	5.32	12.351	43.200	992.568	17.1	0.2	21.0	0.2	−1.0	0.7
AVEL	2057	6.54	14.783	40.912	420.250	17.8	0.2	21.8	0.3	−0.1	1.0
AVZZ	692	3.51	13.446	42.033	725.590	18.6	0.6	22.6	0.7	−4.2	2.4
BAJA	1862	5.57	7.719	43.904	921.789	17.1	0.2	21.6	0.2	−2.3	0.7
BARC	2345	6.94	12.564	46.193	528.451	17.3	0.4	20.5	0.4	1.6	1.6
BARS	1400	4.80	13.582	42.337	1158.059	19.4	0.4	22.3	0.4	−0.9	1.3
BART	1042	3.11	15.018	41.414	689.698	18.9	0.5	23.3	0.5	0.7	1.7
BATE	3866	12.06	12.185	43.709	757.243	17.3	0.1	21.7	0.1	1.0	0.3
BERT	1329	5.64	12.134	44.148	343.660	19.5	0.2	22.6	0.2	−1.3	0.7
BEVA	2354	6.94	13.069	45.672	50.099	17.8	0.2	20.7	0.2	−1.3	1.0
BEVE	1876	5.62	9.769	44.194	144.713	16.4	0.2	20.9	0.2	−0.5	0.7
BGDR	851	2.98	11.895	43.889	740.822	17.9	0.7	21.5	0.7	3.3	2.2
BIEL	3129	11.43	8.048	45.561	480.478	16.0	0.1	20.2	0.1	1.3	1.0
BL01	1647	7.28	12.203	46.137	453.718	17.3	0.2	20.7	0.2	1.5	0.7
BLGN	2333	6.92	11.351	44.511	93.787	18.1	0.3	23.2	0.3	−2.4	1.1
BLRA	2357	8.53	13.560	41.810	419.397	17.2	0.5	20.3	0.8	1.2	1.6
BOBB	1971	7.40	9.383	44.771	370.529	17.5	0.3	21.6	0.2	−1.4	0.8
BOLG	3515	10.55	11.357	44.500	99.743	20.0	0.2	21.5	0.4	−3.4	1.0
BOLO	2409	7.49	11.329	44.488	140.131	17.8	0.4	22.9	0.2	0.7	0.8
BOLZ	886	3.52	11.365	46.497	331.716	16.2	0.4	20.7	0.4	1.9	1.4
BORC	2135	6.32	12.218	46.437	989.399	16.6	0.2	20.5	0.2	0.1	0.8
BORR	2320	7.08	10.696	44.306	1023.384	17.1	0.2	22.6	0.2	0.5	0.5
BOSC	1757	6.07	11.034	45.600	910.495	16.7	0.2	21.0	0.3	0.4	0.5
BOVA	761	3.08	15.911	37.936	73.376	18.4	0.7	22.6	0.6	−0.8	1.9
BRAS	4952	14.55	11.113	44.122	901.198	17.1	0.1	21.4	0.1	1.1	0.2
BRBZ	1453	4.55	11.941	46.797	903.768	16.3	0.2	20.6	0.2	1.0	0.8
BRIS	1708	5.14	11.766	44.225	273.450	19.8	0.2	22.1	0.2	−0.2	0.7
BRSE	1314	4.02	12.084	46.100	381.380	17.6	0.5	19.3	0.4	1.7	1.0
BRU1	1233	3.64	9.725	44.236	172.146	16.0	0.4	21.4	0.3	−0.3	1.0
BSSO	3070	9.51	14.594	41.546	1004.668	18.9	0.2	22.9	0.2	0.6	0.8
BTAC	2132	7.04	11.278	45.258	71.358	17.9	0.2	20.9	0.2	−6.3	0.7
BUCU	5166	14.54	26.126	44.464	143.208	12.5	0.1	22.9	0.1	2.3	0.2
BULG	2671	8.59	15.378	40.078	899.314	18.1	0.1	22.4	0.1	0.3	0.3

Continued

BUSL	1506	4.40	7.152	45.137	496.192	15.8	0.5	20.8	0.4	−0.4	1.3
BUTE	2649	7.55	19.057	47.481	180.789	14.5	0.2	22.2	0.2	0.2	0.6
BZRG	4848	14.54	11.337	46.499	329.117	16.0	0.2	20.4	0.2	1.8	0.6
CA02	1697	6.49	9.000	39.011	69.053	16.6	0.3	21.6	0.3	−0.3	0.8
CA04	1126	5.74	9.134	39.538	253.896	16.9	0.4	21.7	0.4	0.0	1.3
CA05	1339	4.39	9.118	39.238	94.708	16.6	0.2	21.8	0.2	−0.1	0.7
CAFE	3034	9.55	15.237	41.028	1066.318	18.9	0.1	22.1	0.1	1.2	0.3
CAFI	2602	7.78	11.966	43.329	592.573	17.7	0.2	21.0	0.2	0.0	0.5
CAFV	1114	3.36	11.939	45.670	98.418	17.5	0.4	21.5	0.4	0.2	1.0
CALA	2536	7.55	11.164	43.868	117.980	17.7	0.2	22.1	0.2	1.4	0.8
CAMN	1650	5.60	8.281	44.405	390.075	16.1	0.2	20.9	0.2	−0.5	0.8
CAMU	2215	6.95	11.978	43.259	313.253	17.5	0.2	21.5	0.4	−0.3	0.7
CANL	1526	4.40	8.293	44.722	205.512	16.0	0.2	21.0	0.2	−0.6	0.7
CANV	3366	11.16	12.435	46.008	965.915	17.5	0.4	20.0	0.3	−0.1	0.5
CAOC	1644	4.80	13.484	42.290	970.264	19.5	0.4	21.7	0.3	−3.3	0.8
CAR1	1925	6.07	16.211	39.253	678.913	19.1	0.2	23.4	0.3	0.2	0.8
CARG	3121	11.56	10.325	44.112	953.554	16.6	0.2	21.1	0.2	0.2	0.8
CARI	1825	6.52	13.974	41.195	142.348	17.8	0.3	21.3	0.3	−0.8	1.0
CARP	2468	7.53	10.427	45.368	138.811	16.9	0.4	20.8	0.4	0.4	1.0
CARR	846	3.52	10.081	44.069	116.677	16.1	0.8	20.5	0.8	−1.3	1.9
CARZ	2204	7.27	8.680	46.042	1165.291	16.4	0.2	20.4	0.2	1.1	0.7
CASG	1731	6.04	14.941	40.269	90.414	17.7	0.3	21.6	0.3	−0.9	0.8
CASP	2702	8.10	10.865	42.791	374.042	17.4	0.2	19.8	0.2	−1.5	0.4
CAST	2682	8.33	10.405	44.432	755.744	18.0	0.2	21.7	0.2	0.7	0.5
CATU	872	3.52	9.119	45.743	363.723	16.2	0.4	20.5	0.3	1.1	1.1
CDRA	1750	8.62	13.720	42.368	1412.413	19.4	0.4	22.4	0.5	−0.8	1.3
CDRU	2864	8.88	15.305	40.490	1046.456	17.2	0.2	21.0	0.2	1.1	0.4
CECI	1798	5.58	10.527	43.311	75.590	16.6	0.2	21.2	0.2	0.8	0.7
CELI	938	3.75	16.509	39.403	1275.833	18.9	0.3	23.7	0.4	1.3	1.0
CERA	3002	9.00	14.018	41.598	904.376	17.0	0.5	21.1	0.7	1.0	0.7
CERT	3205	9.29	12.982	41.949	765.382	17.0	0.2	20.8	0.2	0.8	0.5
CESI	2915	8.40	12.905	43.005	914.351	17.9	0.2	21.7	0.2	0.8	0.7
CGIA	1488	4.55	12.266	45.207	57.543	16.8	0.2	20.8	0.3	−5.9	0.7
CHAT	868	3.52	7.624	45.753	645.789	15.0	0.7	19.9	0.5	2.0	1.4
CHIG	791	3.52	11.281	45.543	228.102	15.8	0.5	21.3	0.4	−1.0	1.3
CHIV	1759	5.60	9.324	44.320	70.692	16.3	0.2	21.0	0.2	−1.2	0.7

Continued

CIT1	1495	5.32	12.248	43.467	351.495	17.2	0.3	21.5	0.3	0.6	1.1
CITT	1765	6.39	11.795	45.640	97.081	17.5	0.3	20.4	0.3	−3.3	1.1
CIUF	779	3.47	11.628	43.585	360.569	18.0	0.4	21.4	0.5	−1.2	1.4
CODD	1149	3.65	12.112	44.837	46.188	17.6	0.2	21.0	0.2	−5.6	0.7
CODI	2431	7.91	12.112	44.837	45.568	17.5	0.2	21.2	0.2	−2.8	0.5
CODR	2536	8.21	12.979	45.959	91.868	17.6	0.1	21.0	0.1	0.7	0.4
COLI	2507	7.55	9.381	46.139	275.483	16.6	0.4	20.0	0.3	1.8	1.2
COLL	2517	7.93	10.216	44.753	167.352	18.0	0.2	21.2	0.2	0.4	0.5
COLR	1278	3.85	16.422	40.193	766.906	20.1	0.2	23.7	0.3	0.8	0.8
COMO	4394	13.25	9.096	45.802	292.300	16.6	0.2	20.4	0.1	0.5	0.4
CONC	887	3.52	11.009	44.922	64.470	18.5	0.6	21.4	0.5	0.1	2.1
CONI	2120	6.22	13.393	42.412	1239.061	16.7	0.3	22.0	0.3	−2.3	0.7
CONS	2009	7.10	11.832	44.516	51.602	18.7	0.3	22.6	0.3	−7.7	0.9
CORL	2958	9.05	13.304	37.894	662.573	19.5	0.1	21.2	0.1	0.7	0.4
CRAC	2828	9.55	16.435	40.381	360.734	19.6	0.1	23.5	0.1	1.4	0.3
CRMI	2650	8.76	10.980	43.796	586.111	17.6	0.1	22.4	0.2	−0.5	0.4
CRSN	1542	4.40	8.106	45.192	211.678	16.4	0.2	20.1	0.2	−0.2	0.7
CSSB	2659	9.06	12.245	43.209	752.565	17.4	0.1	21.2	0.1	0.4	0.3
CTMG	1311	6.74	11.384	44.573	72.224	20.0	0.4	24.8	0.5	−3.5	1.6
CUCC	2696	8.09	15.816	39.994	669.312	18.8	0.1	21.7	0.2	0.0	0.4
CUOR	1510	4.40	7.648	45.388	483.105	16.0	0.2	20.3	0.2	0.7	0.8
DEMN	1509	4.40	7.293	44.316	862.675	16.3	0.2	21.1	0.2	−1.1	1.0
DEVE	2072	7.29	8.261	46.314	1679.437	16.0	0.4	19.9	0.4	1.0	1.2
DOMS	1507	4.40	8.286	46.119	365.635	15.6	0.2	19.8	0.3	0.9	1.1
EDEN	1418	4.20	14.304	37.523	732.294	20.3	0.3	22.6	0.3	0.6	0.8
EIIV	3074	9.54	15.082	37.514	88.870	18.0	0.2	22.9	0.2	1.6	0.7
ELBA	4378	14.55	10.211	42.753	271.758	16.2	0.1	20.6	0.1	−0.2	0.2
FAEZ	2438	7.11	11.861	44.303	83.836	19.4	0.2	22.1	0.2	−3.7	0.8
FASA	2830	8.33	17.359	40.835	175.765	18.9	0.3	23.6	0.3	−0.2	1.0
FDOS	1201	4.75	11.724	46.304	1889.293	16.0	0.4	20.7	0.2	0.1	0.8
FERA	2381	7.55	11.627	44.814	58.336	17.8	0.2	21.5	0.2	0.0	0.6
FERR	2487	7.98	11.601	44.828	64.523	17.5	0.1	21.7	0.1	0.4	0.4
FIAN	824	3.45	12.588	42.164	188.752	17.1	0.4	21.1	0.4	−0.3	1.0
FIGL	2467	7.55	11.474	43.619	188.037	18.0	0.2	21.4	0.2	0.9	0.6
FIOR	829	3.52	11.585	42.834	753.139	17.3	0.5	21.3	0.6	−0.9	1.5
FIRE	2326	7.55	11.378	44.118	487.576	18.3	0.2	20.8	0.2	1.1	0.7

Continued

FISC	1306	4.06	14.790	40.771	309.956	17.0	0.4	21.2	0.4	−0.7	1.0
FOGG	2749	8.09	15.532	41.452	148.366	18.8	0.3	23.1	0.3	0.3	1.0
FOL1	2245	7.55	12.699	42.955	296.337	18.1	0.2	20.8	0.2	0.4	0.8
FOND	774	3.51	13.415	41.330	61.033	16.2	0.6	21.0	0.5	1.4	1.3
FORL	1106	3.88	12.072	44.198	79.076	20.2	1.2	22.7	1.7	−6.7	2.9
FOSS	2323	7.55	12.807	43.689	176.511	18.9	0.2	23.2	0.2	−0.2	0.6
FRES	2696	8.84	14.669	41.974	404.688	18.7	0.1	23.3	0.1	0.1	0.4
FRMO	1818	5.83	13.731	43.168	259.957	19.3	0.4	23.1	0.4	0.0	1.0
FRRA	2651	9.05	14.292	42.418	92.550	18.6	0.2	22.9	0.2	−0.2	0.7
FUSE	2667	7.85	13.001	46.414	581.908	16.6	0.2	21.1	0.1	0.5	0.4
FVRA	1857	5.77	13.669	37.318	392.526	18.6	0.2	21.0	0.2	0.9	0.8
GALF	2659	8.63	14.567	37.711	731.387	19.2	0.2	20.7	0.2	1.3	0.4
GARI	2048	6.00	12.249	44.677	47.750	17.8	0.4	21.6	0.4	−2.7	1.3
GATE	2045	6.05	14.910	41.513	470.811	19.1	0.2	23.1	0.2	0.2	0.7
GAVO	1737	6.66	10.889	42.937	101.643	17.8	0.4	21.0	0.4	0.7	1.1
GAZZ	2070	6.66	9.829	45.794	441.421	15.9	0.2	20.5	0.2	0.1	0.8
GBLM	3151	10.45	14.026	37.990	1036.374	21.8	0.2	21.8	0.2	0.4	0.5
GENO	4902	14.55	8.921	44.419	155.530	15.9	0.1	20.8	0.1	−0.4	0.1
GENU	1939	5.60	8.959	44.403	127.371	16.4	0.2	21.0	0.2	−1.0	0.7
GEOT	840	3.52	13.511	43.575	119.647	18.7	0.4	22.9	0.4	1.7	1.4
GINE	816	3.52	13.376	43.121	385.195	19.4	0.4	24.0	0.5	−1.3	1.3
GINO	2512	7.47	16.758	40.578	319.137	18.9	0.4	24.1	0.4	3.0	1.3
GIOI	2241	7.05	15.895	38.422	93.074	18.7	0.2	24.2	0.2	0.0	0.8
GIUR	2578	7.47	18.430	40.124	121.857	18.6	0.3	23.8	0.3	0.4	1.0
GNAL	1639	4.84	13.520	42.584	1048.599	17.9	0.4	23.1	0.4	0.9	0.8
GODE	850	3.52	12.385	45.928	112.852	16.5	0.4	20.9	0.4	−2.6	1.1
GORI	2228	6.94	13.624	45.943	153.422	18.2	0.3	20.8	0.2	−0.8	1.1
GOZZ	1509	4.40	8.433	45.747	416.615	15.9	0.2	19.9	0.3	0.6	1.0
GRAM	2124	7.04	13.871	42.976	64.432	17.9	0.2	23.3	0.2	0.0	0.7
GRO1	2197	6.73	15.101	41.067	404.419	18.3	0.2	22.3	0.2	0.9	0.5
GROA	1674	6.64	11.109	42.782	68.056	17.4	0.5	20.5	0.5	1.1	1.6
GROG	2668	8.99	9.892	43.426	241.061	16.5	0.1	21.1	0.1	−0.5	0.3
GROT	3445	10.15	15.060	41.073	499.875	18.2	0.1	22.5	0.1	1.1	0.4
GRZM	2086	7.23	11.148	44.265	602.799	18.6	0.3	21.8	0.3	1.1	0.8
GUAR	3106	9.13	13.312	41.794	718.772	16.1	0.2	20.5	0.2	0.8	0.4
GUAS	2352	7.80	10.662	44.918	69.983	17.1	0.1	21.0	0.1	−1.1	0.4

Continued

GUB2	2407	7.55	12.578	43.351	544.638	17.4	0.5	20.8	0.5	1.8	1.6
GUMA	2291	7.27	13.335	43.063	651.612	18.8	0.2	23.6	0.2	−0.1	0.8
HELM	981	3.26	12.385	46.716	2451.269	15.9	0.4	20.4	0.4	−0.9	1.3
HMDC	2582	9.05	14.783	36.959	586.583	20.1	0.1	20.9	0.2	−0.5	0.5
IENG	3879	11.62	7.639	45.015	316.619	15.7	0.1	20.5	0.1	0.2	0.2
IGLE	2364	7.05	8.533	39.311	283.047	17.2	0.2	22.1	0.2	1.5	0.8
IGMI	2864	8.61	11.214	43.796	95.058	18.0	0.2	21.5	0.2	0.0	0.7
IMOL	967	3.14	11.713	44.353	114.541	19.9	0.4	22.4	0.3	−1.4	1.1
IMP3	1688	5.00	8.014	43.873	86.742	15.3	0.4	21.0	0.3	0.5	0.8
INGR	4486	13.47	12.515	41.828	104.447	17.0	0.2	20.4	0.2	0.6	0.5
ISCH	2594	7.98	15.897	41.904	373.486	18.9	0.3	23.6	0.3	1.1	1.0
ISER	2048	6.99	14.236	41.600	550.741	18.3	0.5	22.7	0.5	0.7	1.6
ITIM	2060	8.37	11.718	44.348	98.089	18.7	0.2	22.9	0.2	−0.9	0.5
ITRA	2030	10.51	14.002	42.659	105.440	18.9	0.3	23.0	0.3	−1.0	1.2
ITRN	2127	7.32	12.582	44.048	57.744	19.2	0.2	22.5	0.2	−0.5	0.5
JOAN	2754	8.06	13.416	46.184	1190.456	17.2	0.1	20.8	0.1	0.0	0.4
JOPP	2928	8.87	15.886	38.607	553.819	18.6	0.1	23.7	0.1	0.4	0.4
KNJA	638	3.18	22.255	43.567	291.064	12.1	0.8	24.0	0.7	2.0	2.4
LAGA	2532	8.39	10.947	44.078	757.985	17.7	0.4	21.5	0.2	−0.2	0.9
LAME	837	3.08	16.235	38.878	54.485	19.0	0.6	23.5	0.5	1.6	1.8
LANU	2198	7.29	9.548	39.883	510.315	15.7	0.2	21.5	0.3	−0.1	0.8
LARI	1985	7.53	14.922	41.810	434.758	19.0	0.2	23.5	0.3	0.5	0.8
LASP	3054	9.07	9.840	44.073	87.143	16.4	0.1	21.1	0.1	−0.4	0.3
LAT1	2538	7.54	12.901	41.471	97.943	16.9	0.2	21.2	0.2	5.3	1.7
LDNS	864	3.04	10.827	45.167	81.086	16.5	0.7	21.4	0.8	0.2	2.2
LEGN	1962	6.47	11.269	45.184	71.268	17.1	0.4	21.4	0.4	1.3	1.1
LERO	1909	5.72	11.957	45.346	67.548	16.9	0.5	21.4	0.4	−1.5	1.5
LINZ	2605	7.55	14.283	48.310	335.084	15.5	0.2	20.6	0.2	1.2	0.8
LMPR	868	3.46	10.891	43.811	112.430	18.0	0.4	21.7	0.5	−0.3	1.4
LNSS	3087	9.14	13.040	42.603	1150.857	17.8	0.2	21.7	0.2	−0.1	0.6
LOAN	1899	5.60	8.250	44.119	70.767	15.9	0.2	20.9	0.2	−0.4	0.8
LOCR	732	2.84	16.240	38.236	74.932	18.9	0.8	23.7	0.8	−0.2	2.2
LPEL	2105	7.26	14.183	42.047	816.469	19.2	0.4	24.7	0.7	−1.2	1.6
LUCE	1330	4.13	15.335	41.514	278.357	19.3	0.2	23.3	0.3	−0.1	0.8
M0SE	3610	10.76	12.493	41.893	120.573	16.9	0.2	20.3	0.2	−0.9	0.7
MABZ	1473	4.55	10.551	46.686	1092.071	16.0	0.3	21.0	0.3	2.3	0.8

Continued

MACE	2345	7.55	13.451	43.294	307.111	19.3	0.2	23.8	0.2	−0.5	0.6
MACO	2064	7.55	8.770	40.269	637.708	17.7	0.2	21.6	0.2	1.8	0.8
MADA	1749	5.11	10.366	43.748	56.867	16.4	0.2	21.2	0.2	−0.1	0.8
MAGL	745	3.52	13.588	43.138	310.111	19.2	0.4	24.5	0.5	−0.9	1.5
MANO	1024	3.10	14.059	42.273	192.080	19.4	0.5	22.1	0.5	−2.5	2.2
MAON	2870	9.22	11.131	42.428	228.386	16.1	0.1	21.0	0.1	0.0	0.4
MARG	1131	3.40	9.767	45.571	207.066	16.2	0.4	20.0	0.4	1.6	1.4
MARI	839	3.52	11.868	42.036	80.008	17.1	0.4	20.8	0.4	−0.5	1.0
MARO	805	3.52	11.669	45.748	158.145	16.1	0.4	20.4	0.4	−0.1	1.0
MARS	4317	14.55	5.354	43.279	61.813	16.1	0.2	19.9	0.2	−0.4	0.6
MAT1	4913	14.20	16.705	40.649	534.520	18.7	0.2	23.4	0.1	0.5	0.4
MATE	5119	14.55	16.705	40.649	535.647	19.4	0.1	23.3	0.1	0.7	0.2
MATG	1053	3.46	16.705	40.649	535.597	20.2	0.4	23.3	0.3	−0.1	0.9
MCEL	2714	8.59	15.802	40.326	1058.870	19.9	0.1	23.2	0.1	0.1	0.4
MCIN	1703	5.24	11.489	43.058	612.898	17.2	0.3	21.1	0.3	0.0	1.3
MCRV	2937	9.99	15.168	40.783	1175.170	18.2	0.2	23.0	0.2	1.5	0.4
MDEA	3710	12.48	13.436	45.925	165.698	18.2	0.1	20.8	0.1	−0.5	0.4
MEDI	4882	14.55	11.647	44.520	50.035	17.7	0.2	22.4	0.4	−1.3	0.5
MELA	2563	7.52	15.127	41.706	162.948	19.7	0.2	23.1	0.2	−0.4	0.5
MFUS	1009	3.67	14.834	41.058	615.298	18.2	0.3	21.1	0.3	−1.2	0.9
MGAB	2387	7.29	12.111	42.913	532.573	17.3	0.2	20.7	0.2	0.7	0.5
MLAG	858	2.91	12.779	43.431	866.568	20.6	0.6	24.1	0.9	2.1	2.0
MLFT	1391	4.47	16.604	41.196	85.649	19.3	0.2	23.1	0.2	0.0	0.8
MMNO	1332	3.83	15.972	39.870	1013.482	17.9	0.6	20.1	0.7	2.5	1.5
MNIA	1005	2.90	16.687	40.365	158.271	19.4	0.5	23.1	0.4	0.0	1.7
MO01	2553	9.21	10.900	44.641	94.916	18.6	0.1	22.2	0.1	−4.4	0.6
MO02	3041	12.30	10.835	44.340	740.075	18.4	0.1	22.2	0.1	1.0	0.4
MO03	2028	9.22	10.625	44.360	837.512	19.1	0.1	22.0	0.1	0.3	0.5
MO05	2213	9.01	11.286	44.838	64.183	18.1	0.4	21.3	0.2	1.2	0.7
MOCA	755	3.36	11.143	46.098	1147.213	16.8	0.5	22.0	0.5	0.9	1.9
MOCO	2869	8.75	15.159	41.371	1072.633	19.4	0.2	22.9	0.2	0.0	0.4
MODE	3001	8.62	10.949	44.629	92.171	19.6	0.1	21.4	0.1	−3.8	0.4
MODR	2615	8.93	13.881	41.146	375.608	16.9	0.1	20.6	0.1	0.3	0.4
MOGG	2377	6.94	13.198	46.407	377.975	17.0	0.2	20.9	0.2	1.4	0.8
MONC	2866	9.24	7.927	45.074	464.456	15.9	0.1	20.8	0.1	−0.5	0.6
MONF	865	3.52	8.453	45.134	177.743	16.6	0.5	20.8	0.4	−1.5	1.3

Continued

MONT	866	3.52	7.709	45.387	413.503	15.9	0.4	19.7	0.5	1.0	1.1
MONV	1521	4.40	7.829	44.390	637.697	15.8	0.3	21.0	0.2	−0.7	0.8
MONZ	1663	4.80	9.272	45.577	227.205	15.9	0.2	20.8	0.2	−0.2	0.8
MOPI	2434	7.53	17.274	48.373	578.978	15.0	0.3	21.3	0.3	0.0	1.3
MOPS	2885	8.29	10.949	44.629	92.203	19.0	0.1	21.8	0.1	−2.7	0.5
MORB	2517	7.55	9.567	46.134	325.059	16.0	0.3	20.4	0.2	2.0	0.9
MORO	2120	7.10	12.619	42.053	201.594	17.2	0.2	20.6	0.3	0.3	0.7
MOST	861	2.87	16.574	38.439	60.310	19.2	0.6	24.6	0.6	1.2	1.8
MOZ2	3245	9.22	10.544	43.979	156.754	17.3	0.2	21.4	0.2	−0.6	1.1
MPRA	4203	12.53	12.988	46.241	808.564	16.5	0.2	20.6	0.1	−0.1	0.3
MRGE	2675	8.86	7.061	45.770	1722.774	15.4	0.2	19.7	0.2	0.2	0.7
MRLC	3238	9.65	15.489	40.756	631.484	19.9	0.2	23.9	0.1	1.2	0.4
MRRA	2621	8.67	13.916	42.885	61.886	18.9	0.2	23.6	0.2	−1.0	0.7
MRVN	2732	9.17	16.196	41.061	593.655	19.7	0.1	23.3	0.1	0.7	0.3
MSAG	2879	9.15	15.910	41.712	881.257	19.1	0.1	23.3	0.1	0.1	0.3
MSEL	3603	10.86	11.647	44.520	49.272	18.4	0.1	22.0	0.1	−1.5	0.3
MSRU	2620	8.48	15.508	38.264	396.749	20.1	0.1	23.3	0.1	−1.3	0.4
MT01	2106	6.33	12.201	45.749	98.576	17.7	0.2	20.6	0.2	0.7	0.7
MTRA	2100	9.07	13.240	42.528	995.834	19.0	0.6	22.3	0.5	0.5	1.7
MTSN	2448	8.59	15.751	40.266	1132.323	19.2	0.1	23.2	0.1	1.1	0.4
MTTG	2558	9.52	15.700	38.003	544.100	18.1	0.2	23.9	0.1	0.7	0.4
MTTO	2756	10.01	12.993	42.456	1738.067	16.7	0.2	21.8	0.3	0.3	0.7
MUR1	948	2.91	12.525	43.263	883.051	18.0	0.8	21.8	0.9	1.8	2.1
MURA	1259	4.03	9.566	39.424	67.838	16.3	0.4	22.5	0.4	3.1	1.3
MVAL	3109	9.06	12.407	43.382	638.322	17.6	0.1	21.5	0.1	0.9	0.3
NAPO	1972	6.54	14.276	40.870	127.707	18.1	0.2	23.5	0.2	0.0	0.8
NERO	851	3.52	8.455	45.712	380.995	15.7	0.4	20.6	0.5	0.3	1.1
NETT	752	3.48	12.648	41.461	100.197	16.9	0.3	21.4	0.4	−1.1	0.9
NICO	1688	5.55	14.327	41.047	100.766	17.7	0.2	22.0	0.3	−0.3	0.8
NOCI	3034	9.98	17.064	40.789	437.667	19.3	0.1	24.3	0.1	1.4	0.3
NOT1	4928	14.55	14.990	36.876	126.342	19.9	0.1	21.4	0.1	−0.4	0.1
NOVE	2004	6.15	12.588	45.668	47.962	17.9	0.4	21.1	0.4	−2.4	1.1
NOVR	1537	4.40	8.614	45.447	218.628	16.7	0.2	20.8	0.2	0.2	0.7
NPAZ	859	3.86	20.519	43.140	549.504	14.1	0.2	23.6	0.2	0.8	0.8
NU01	1470	7.14	9.313	40.315	586.715	16.9	0.4	21.6	0.4	0.4	1.3
OATO	2276	7.24	7.765	45.042	658.824	15.5	0.2	20.6	0.2	0.6	0.5

Continued

OCRA	2270	8.57	13.039	42.050	878.220	17.2	0.3	20.3	0.4	1.0	0.9
ODEZ	1505	4.38	12.489	45.788	70.431	17.7	0.2	21.1	0.2	−1.2	0.7
OLGI	2379	7.30	12.355	42.055	207.877	17.5	0.2	20.6	0.3	0.0	0.7
OMBR	3396	12.06	11.560	43.733	1093.388	17.4	0.1	21.3	0.1	0.2	0.2
ORID	4762	14.55	20.794	41.127	773.006	11.6	0.1	24.0	0.1	0.3	0.4
ORZI	704	3.52	9.921	45.409	132.538	16.0	0.4	21.2	0.4	−0.9	1.3
OSIM	839	3.48	13.482	43.481	195.886	18.8	0.4	23.5	0.4	0.8	1.4
OTRA	1414	6.58	13.646	41.955	729.191	18.6	0.7	22.3	0.5	−1.6	1.6
OVRA	2635	8.67	13.515	42.138	1432.100	19.6	0.5	21.4	0.5	−0.3	1.3
PACA	3511	12.21	14.556	40.871	128.104	17.0	0.1	21.0	0.1	−1.1	0.2
PADO	4395	13.64	11.896	45.411	64.712	16.7	0.1	20.8	0.1	−1.2	0.3
PAGA	717	3.52	13.466	42.362	716.999	16.6	0.5	22.1	0.5	−4.0	1.5
PAGL	1779	5.27	14.498	42.164	287.607	19.2	0.2	22.6	0.2	−0.4	0.8
PALA	1760	7.07	9.897	45.602	238.747	16.3	0.4	20.2	0.4	2.2	1.5
PALZ	2765	8.59	15.960	40.944	497.679	19.7	0.1	23.1	0.1	0.3	0.4
PAOL	1835	5.58	14.568	41.031	714.571	17.5	0.4	21.2	0.7	0.2	1.1
PARM	3036	8.76	10.312	44.765	121.827	17.9	0.2	21.7	0.2	0.7	0.6
PARO	2234	7.28	8.081	44.446	849.772	15.9	0.2	21.1	0.2	0.6	0.5
PARR	2122	6.54	11.123	45.777	875.755	16.8	0.3	20.8	0.3	0.1	1.0
PASS	2117	6.25	11.902	46.193	1418.690	16.6	0.3	20.1	0.3	0.4	0.7
PAUN	1180	3.55	13.349	38.106	113.504	20.5	0.4	21.9	0.5	1.1	1.3
PAZO	2396	7.55	13.053	45.806	50.089	17.3	0.2	20.8	0.2	0.1	0.5
PBRA	2531	9.07	14.229	42.124	571.948	19.6	0.3	22.7	0.3	0.0	0.9
PEJO	2188	6.54	10.676	46.363	1612.677	15.7	0.4	21.0	0.3	0.9	0.9
PENC	5020	14.54	19.282	47.790	291.737	14.7	0.1	22.0	0.1	0.0	0.4
PES2	1933	5.87	12.893	43.893	66.881	18.7	0.3	22.6	0.2	1.7	0.9
PESA	805	3.52	12.918	43.901	59.296	19.3	0.3	22.9	0.4	−0.1	1.2
PESC	722	3.46	14.201	42.470	71.212	19.1	0.3	23.0	0.4	−0.8	1.0
PESR	1246	3.96	12.841	43.941	201.379	20.5	0.6	23.5	0.5	−0.2	0.8
PFA2	2499	7.55	9.785	47.515	1090.095	16.0	0.2	20.2	0.2	0.8	0.8
PFER	1323	4.54	10.295	42.793	71.979	16.7	0.8	21.0	0.7	−0.7	2.1
PIAC	2381	7.93	9.690	45.043	115.082	17.6	0.2	21.0	0.1	0.1	0.5
PIBI	1146	3.39	12.453	43.128	258.961	16.8	0.4	20.8	0.5	−0.4	1.4
PIC1	2406	7.55	9.690	45.043	115.304	17.5	0.2	20.9	0.2	1.5	0.6
PIET	2821	9.05	12.402	43.451	745.467	17.9	0.1	21.6	0.1	1.0	0.3
PIGN	1265	3.93	14.180	41.200	397.457	17.9	0.3	21.6	0.2	−0.7	0.8

Continued

PILA	1468	4.55	11.906	46.566	2141.701	15.8	0.6	20.6	0.5	1.1	1.4
PIOB	870	3.52	12.482	43.612	448.001	18.9	0.5	22.9	0.4	0.7	1.3
PIPA	2570	8.25	16.816	39.485	478.963	18.8	0.1	24.0	0.1	1.2	0.4
PITI	1720	5.50	11.673	42.634	392.020	16.7	0.4	20.9	0.4	0.3	1.0
PLAC	3045	9.84	16.438	38.449	594.660	18.4	0.1	24.1	0.1	1.1	0.4
POFI	2740	8.31	13.712	41.717	850.419	17.0	0.3	21.5	0.2	1.6	0.7
POGG	2650	8.15	16.254	40.917	520.863	19.1	0.3	23.4	0.3	0.4	1.0
PORD	2397	6.94	12.661	45.957	81.764	17.0	0.4	20.5	0.2	−0.1	0.8
POZL	1129	3.51	14.794	36.729	90.654	20.5	0.4	21.6	0.4	0.2	1.1
POZZ	2186	6.55	11.682	46.423	1392.505	16.5	0.2	20.7	0.2	0.8	0.7
PRAI	820	2.99	15.780	39.897	59.793	18.3	0.6	19.8	0.8	0.7	1.9
PRAT	4630	14.55	11.099	43.886	119.966	17.3	0.1	21.4	0.1	0.1	0.1
PREM	1964	6.76	9.878	45.870	671.999	16.1	0.3	20.5	0.2	0.7	0.7
PRET	1489	4.55	12.073	47.029	1912.767	15.2	0.7	21.7	0.5	0.1	1.3
PRIG	1096	4.54	15.109	40.312	134.092	17.9	1.0	21.6	0.8	−0.7	3.2
PRTG	3032	6.94	12.833	45.767	59.527	18.2	0.3	21.1	0.3	−2.3	4.3
PSAN	1736	6.61	14.139	42.519	62.214	18.3	0.2	23.1	0.2	−1.3	0.7
PSB1	2831	9.31	14.811	41.223	588.324	18.1	0.1	22.3	0.1	0.5	0.4
PSST	798	3.52	11.120	42.428	72.275	16.8	0.5	20.9	0.4	−2.3	1.4
PSTE	2050	7.55	11.120	42.428	72.366	16.4	0.3	21.1	0.2	−0.3	0.8
PTNZ	1296	4.13	15.817	40.635	731.144	20.2	0.5	23.6	0.5	0.3	1.4
PTO1	1728	4.99	12.334	44.952	49.312	17.0	0.2	21.1	0.2	−4.8	0.6
PTRJ	2500	9.00	14.529	41.364	1113.089	17.5	0.2	22.9	0.2	0.9	0.5
PTRP	2347	8.04	16.061	40.532	828.710	19.2	0.2	23.7	0.2	1.1	0.5
RAFF	2535	9.52	14.362	37.223	300.671	20.2	0.1	21.0	0.1	−0.6	0.3
RAMS	1742	5.38	10.278	44.411	851.642	17.6	0.4	21.7	0.2	0.2	0.7
RAPA	738	3.41	9.221	44.355	70.378	15.7	0.5	21.6	0.5	−0.3	1.3
RASS	2882	9.22	11.836	43.647	354.035	17.5	0.2	20.9	0.1	0.3	0.5
RAVE	2941	10.12	12.200	44.413	54.814	18.6	0.1	23.0	0.1	−3.9	0.2
RAVS	2475	8.44	12.192	44.405	51.801	18.5	0.3	22.9	0.2	−4.0	0.7
RDPI	2439	8.85	12.710	41.760	816.706	17.6	0.3	20.9	0.4	2.5	0.8
RE01	2280	9.22	10.640	44.887	69.778	16.4	0.1	22.3	0.1	−2.7	0.5
REBO	1435	5.16	12.030	45.196	58.199	17.0	0.2	21.1	0.2	−1.6	0.6
REGG	2174	7.29	10.637	44.706	103.569	18.1	0.2	23.3	0.2	−1.6	0.5
RESU	2090	7.35	14.057	37.647	782.470	18.0	0.2	22.2	0.2	0.8	0.6
RIET	2525	7.55	12.857	42.408	457.221	17.0	0.2	20.9	0.3	0.8	0.8

Continued

RMPO	3043	9.07	12.703	41.811	449.666	17.5	0.2	21.3	0.2	0.3	0.5
RNI2	3700	10.94	14.152	41.704	1017.953	18.4	0.2	22.3	0.2	1.0	0.5
ROGA	3825	11.89	10.340	44.207	1311.571	16.6	0.1	20.8	0.1	−0.7	0.2
RONC	2210	6.55	10.670	45.984	885.439	16.4	0.2	20.3	0.2	0.5	0.7
ROPI	2168	6.28	13.337	42.332	991.841	17.3	0.5	21.8	0.5	−2.1	0.8
ROSS	978	3.08	16.641	39.600	96.204	20.6	0.6	24.6	0.6	−0.2	1.6
ROVE	3189	9.38	11.042	45.894	261.771	17.3	0.1	20.7	0.1	0.9	0.5
ROVI	2247	6.90	11.783	45.087	62.783	18.0	0.2	21.4	0.2	−0.7	0.5
ROVR	2165	6.77	11.072	45.647	1365.924	17.1	0.2	21.3	0.2	0.6	0.5
RSMN	3179	9.64	12.451	43.934	767.430	19.2	0.2	23.3	0.1	−0.3	0.5
RSPX	3025	9.17	7.265	45.148	1323.230	15.8	0.1	20.7	0.1	0.9	0.4
RSTO	4003	12.55	14.002	42.658	102.583	18.8	0.2	23.2	0.2	−0.5	0.4
SABA	928	3.86	19.697	44.760	140.883	14.6	0.3	24.0	0.4	1.7	0.9
SACR	3126	10.54	14.706	41.398	847.043	17.6	0.2	21.6	0.2	1.8	0.3
SALA	1690	5.54	15.557	40.417	504.518	18.3	0.3	23.2	0.5	1.0	1.1
SALB	1947	6.05	16.346	39.877	1187.635	20.0	0.3	24.0	0.3	1.1	0.7
SALO	3166	9.69	10.524	45.618	589.067	15.9	0.2	21.1	0.2	−0.9	0.6
SAPP	1955	6.41	12.690	46.567	1329.481	16.6	0.2	20.8	0.2	2.1	0.7
SAPR	1849	7.32	15.630	40.074	65.370	17.7	0.2	21.8	0.2	−0.4	0.8
SAQU	2029	6.18	8.399	44.292	118.029	16.0	0.4	20.7	0.4	−1.3	1.0
SARN	2202	6.54	11.142	46.419	1049.694	16.5	0.2	20.7	0.2	0.8	0.6
SASA	2532	8.17	17.965	40.385	99.264	18.5	0.3	23.8	0.3	−0.8	1.0
SASO	1077	4.94	11.822	43.928	824.938	20.2	1.0	23.3	0.9	−0.7	3.1
SASS	1964	7.55	8.567	40.721	302.460	16.4	0.3	21.3	0.3	2.2	0.9
SAVI	1685	5.29	7.661	44.648	380.441	16.2	0.2	20.5	0.2	−0.7	0.7
SBG2	2574	7.46	13.110	47.803	1323.363	15.9	0.2	20.7	0.2	1.2	0.7
SBPO	3081	9.15	10.920	45.051	62.434	17.0	0.1	20.8	0.1	0.3	0.4
SCHI	2357	7.15	11.363	45.718	254.628	16.9	0.2	20.8	0.2	0.2	0.9
SCHR	2431	9.84	16.085	40.190	859.448	19.2	0.1	23.6	0.1	1.3	0.4
SCRA	2593	8.65	14.002	42.268	166.548	20.3	0.2	22.6	0.2	−0.3	0.7
SCTE	2725	9.45	18.467	40.072	143.208	18.8	0.1	23.7	0.1	−0.1	0.3
SDNA	2207	6.90	12.564	45.630	66.745	17.4	0.2	21.0	0.2	−1.8	0.5
SEAN	699	3.42	11.026	43.831	94.301	17.5	1.0	21.8	0.7	−2.1	2.2
SENI	797	3.52	13.215	43.708	65.047	19.0	0.3	23.0	0.3	0.2	1.0
SERM	2501	7.55	11.300	45.007	67.995	17.5	0.2	22.4	0.2	0.2	0.5
SERR	1518	4.40	8.853	44.731	251.173	16.7	0.2	21.0	0.2	0.1	0.7

Continued

SERS	2802	8.84	16.689	39.036	1214.970	18.5	0.1	24.5	0.1	0.7	0.4
SEVI	1701	5.18	7.837	45.535	323.494	15.4	0.3	20.2	0.3	1.2	1.0
SGIO	809	3.52	11.802	45.601	91.982	16.7	0.5	20.4	0.5	−0.5	1.6
SGIP	3401	10.36	11.183	44.636	63.496	17.7	0.2	22.7	0.2	−5.4	0.4
SGL1	1960	6.03	13.766	41.407	100.679	17.0	0.4	22.3	0.4	3.7	1.8
SGRE	1968	6.18	13.501	42.336	808.381	17.9	0.5	20.9	0.4	−2.5	1.2
SGRT	2884	9.15	15.744	41.755	949.239	20.0	0.2	23.7	0.1	0.7	0.4
SGTA	3032	9.49	15.365	41.136	716.892	19.5	0.1	23.0	0.1	1.0	0.3
SIEN	3120	11.60	11.338	43.315	386.652	16.8	0.1	20.8	0.1	0.5	0.3
SILA	860	3.52	10.785	46.625	753.937	16.0	1.9	21.5	1.3	2.1	6.7
SIN2	1725	5.62	9.692	40.574	104.334	16.5	0.4	21.8	0.5	0.2	1.1
SIRC	1920	5.64	15.282	37.076	90.443	20.2	0.2	21.8	0.2	−1.9	0.7
SIRI	2706	8.59	15.866	40.184	1144.171	19.6	0.1	24.1	0.2	−0.4	0.4
SLCN	2712	10.13	15.633	40.391	1048.759	18.1	0.1	23.2	0.1	0.8	0.4
SMRA	2596	9.07	13.924	42.048	474.097	19.5	0.3	23.0	0.2	−2.4	1.0
SNAL	3215	10.55	15.209	40.926	865.647	18.0	0.1	22.4	0.1	1.2	0.3
SOFI	4478	14.36	23.395	42.556	1119.535	11.9	0.1	23.6	0.2	0.0	0.5
SONA	816	3.52	10.828	45.445	180.903	17.0	0.5	21.2	0.4	−1.8	1.6
SORR	1350	4.00	14.396	40.629	131.733	17.6	0.7	21.9	0.8	0.5	1.6
SOV1	1273	4.10	16.547	38.684	61.634	18.3	0.3	24.5	0.4	0.6	1.1
SPCI	2716	8.19	15.260	41.740	244.448	18.4	0.3	23.5	0.3	1.0	1.0
SPER	2122	6.55	11.509	46.069	604.829	16.6	0.2	20.6	0.2	0.5	0.6
SPRN	2653	7.55	16.583	47.684	278.854	15.8	0.2	22.3	0.2	−0.6	0.6
STBZ	1455	4.55	11.426	46.898	1043.752	16.0	0.2	21.0	0.2	2.2	0.9
SUSE	1031	4.08	12.209	45.857	221.733	17.7	0.5	20.6	0.5	−0.9	2.9
SVTO	2786	8.59	16.441	40.604	493.614	19.4	0.1	23.3	0.1	0.6	0.3
TAMB	1205	3.87	12.396	46.061	1117.585	15.8	0.4	21.4	0.4	0.9	1.1
TAOR	2210	7.05	15.289	37.853	250.563	19.7	0.4	21.1	0.4	0.7	1.0
TARA	1454	4.57	17.284	40.527	126.559	20.0	0.3	23.4	0.2	−0.4	0.8
TARO	2472	8.00	9.766	44.488	473.618	17.1	0.2	21.5	0.3	0.6	0.9
TARQ	1773	5.38	11.758	42.254	185.665	16.4	0.5	20.7	0.5	1.3	1.9
TARV	2357	6.94	13.593	46.502	761.144	17.0	0.3	21.2	0.2	2.3	1.0
TELI	829	3.47	15.010	41.972	62.303	18.0	0.6	25.5	0.6	−9.5	1.6
TEMP	2234	7.05	9.100	40.908	597.268	16.6	0.2	21.8	0.2	1.0	0.7
TEOL	3371	10.27	11.677	45.343	203.405	17.9	0.2	20.8	0.2	0.1	0.5
TERA	1778	6.48	13.700	42.662	333.339	20.6	0.4	23.6	0.4	−1.5	1.3

Continued

TERI	2010	7.46	12.650	42.567	209.799	17.5	0.4	20.1	0.5	0.1	1.2
TGPO	2178	6.89	12.228	45.003	49.355	17.4	0.2	21.3	0.2	−5.1	0.6
TGRC	937	3.08	15.651	38.108	139.230	19.4	0.6	23.4	0.6	1.7	1.8
TITO	2225	6.54	15.724	40.601	818.203	19.0	0.3	23.3	0.3	0.4	0.7
TLSE	4945	14.53	1.481	43.561	207.186	16.3	0.1	19.5	0.1	0.5	0.4
TOIR	1874	5.78	8.212	44.124	106.636	16.2	0.3	21.1	0.2	−1.6	1.1
TOLF	3226	10.34	12.000	42.064	362.759	17.1	0.1	20.7	0.2	−0.4	0.4
TORC	823	3.52	7.641	45.017	301.121	16.0	0.4	20.9	0.4	1.5	1.1
TORI	4800	14.55	7.661	45.063	310.746	15.9	0.1	20.1	0.1	0.6	0.2
TREB	996	3.08	16.527	39.869	138.358	20.0	0.6	24.0	0.6	2.0	1.6
TREC	3500	11.70	10.018	44.337	490.707	16.8	0.2	20.8	0.2	−0.3	0.5
TREN	2090	6.54	11.118	46.091	275.298	16.4	0.2	21.1	0.2	−0.2	0.7
TREV	2025	6.28	12.222	45.680	78.194	17.2	0.2	20.9	0.2	−0.2	0.5
TRI0	2183	6.94	13.788	45.661	161.608	17.9	0.2	20.9	0.3	0.5	0.7
TRIE	4183	12.44	13.764	45.710	323.409	17.8	0.1	20.3	0.1	0.2	0.3
TRIV	3321	10.35	14.550	41.767	599.357	18.9	0.1	23.7	0.1	0.6	0.3
TRLU	3826	12.30	11.267	43.609	461.460	17.4	0.1	21.6	0.1	0.2	0.1
UDI1	3055	9.19	13.253	46.038	149.175	17.7	0.1	20.8	0.1	0.0	0.2
UDIN	2124	6.94	13.228	46.055	180.643	17.5	0.2	20.8	0.3	−0.1	0.8
UGEN	2757	8.18	18.162	39.928	152.185	18.6	0.3	23.8	0.2	0.2	0.9
UMBE	2887	9.67	12.329	43.311	305.639	17.4	0.1	21.4	0.1	2.8	0.4
UNPA	1022	3.28	13.348	38.106	103.371	19.7	0.6	22.0	0.7	2.3	1.8
UNPG	4719	14.55	12.356	43.119	351.097	17.2	0.1	21.0	0.2	−0.4	0.4
UNTR	2687	10.53	12.674	42.559	219.147	17.6	0.5	20.6	0.4	−0.3	0.9
USAL	1897	5.39	18.112	40.335	69.194	19.1	0.2	23.9	0.2	−0.5	0.6
VAGA	2922	9.35	14.234	41.415	784.814	16.1	0.4	21.0	0.2	0.7	0.4
VALC	2583	8.29	12.285	43.279	663.122	17.5	0.1	21.2	0.2	0.6	0.4
VALD	1296	4.25	11.998	45.898	299.100	16.0	0.4	21.4	0.4	−1.2	0.8
VALE	2751	8.00	16.905	41.016	207.261	18.8	0.3	23.5	0.2	0.4	0.8
VARE	1515	4.88	8.829	45.814	443.103	16.0	0.2	20.5	0.2	0.4	0.8
VELO	1943	6.19	11.367	45.789	405.238	16.1	0.2	20.9	0.2	−1.0	0.8
VEN1	2268	7.07	12.354	45.431	60.434	15.9	0.2	21.2	0.2	−1.9	0.5
VENO	1724	5.26	15.809	40.967	467.786	19.8	0.4	23.6	0.3	−0.1	0.8
VENT	3204	9.46	13.422	40.795	112.550	17.2	0.1	21.2	0.1	−0.9	0.3
VERB	807	3.52	8.567	45.941	282.232	15.9	0.4	20.3	0.4	2.7	1.4
VERG	2583	7.86	11.111	44.287	271.953	17.4	0.2	23.3	0.2	1.0	0.5

Continued

VERL	1745	5.28	8.421	45.331	183.933	16.1	0.2	20.6	0.3	−1.0	1.0
VERO	2465	7.55	11.002	45.445	123.795	16.0	0.4	20.9	0.4	0.8	1.1
VGAR	1465	4.46	15.962	41.893	514.121	19.4	0.3	23.5	0.2	−0.8	1.0
VICE	2163	6.90	11.556	45.564	96.172	16.8	0.2	20.8	0.2	−0.9	0.6
VIGG	1155	3.84	16.116	39.986	954.632	19.1	0.7	24.0	0.8	1.9	1.6
VILL	4993	14.55	356.048	40.444	647.348	16.4	0.2	19.2	0.2	0.5	0.5
VILS	1652	7.24	9.521	39.143	101.727	16.9	0.4	22.0	0.6	0.0	1.3
VINC	640	3.47	14.562	41.468	571.570	18.4	0.7	23.4	0.5	−0.1	1.6
VIT1	1743	5.38	12.103	42.426	405.640	16.8	0.2	21.1	0.2	0.8	0.7
VITE	719	3.52	12.112	42.419	418.740	16.6	0.4	20.3	0.4	0.1	1.2
VITT	1168	3.40	12.301	45.993	194.645	17.0	0.5	21.4	0.4	−0.1	1.1
VLPN	766	3.52	10.852	43.006	207.284	16.9	0.3	21.3	0.3	0.3	1.0
VLSG	2661	9.54	15.642	38.224	117.389	18.5	0.2	23.2	0.1	0.5	0.3
VMIG	1011	3.12	7.651	43.786	70.322	15.9	0.7	20.2	1.0	0.0	1.4
VR02	2033	7.14	10.994	45.438	127.491	16.4	0.3	21.1	0.2	1.3	0.8
VRRA	1983	6.11	10.865	43.401	597.854	16.7	0.3	21.9	0.3	0.5	1.1
VTRA	2673	9.05	14.708	42.110	209.780	18.3	0.2	22.8	0.2	−1.0	0.7
VULT	2736	9.91	15.616	40.955	1082.214	19.6	0.1	23.4	0.1	0.6	0.3
VVLO	4506	14.54	13.623	41.870	1045.769	18.0	0.2	21.6	0.2	1.4	0.7
WTZR	5118	14.54	12.879	49.144	666.028	15.3	0.2	20.4	0.2	0.6	0.5
ZAGA	984	3.52	12.748	41.862	198.420	17.3	0.4	21.0	0.5	−0.3	1.1
ZERI	2573	9.48	9.752	44.388	1448.007	16.3	0.2	21.1	0.1	−0.5	0.4
ZOUF	3923	12.18	12.974	46.557	1946.492	16.4	0.1	21.0	0.1	2.0	0.2